Biochar Rewires Root Exudates and the Rhizosphere Microbiome and Its Functionality

Hanyue Yang[1], Amina Furrkukh Mughal[2], Yaqi You[1,*]

[1]Department of Environmental Resources Engineering, SUNY College of Environmental Science and Forestry

[2]Graduate Program in Environmental Science, SUNY College of Environmental Science and Forestry

*Correspondence:

Yaqi You

402 Baker Lab, 1 Forestry Dr, Syracuse, NY 13210

E-mail: yyou@esf.edu

Phone: +1-315-470-6765

ABSTRACT

Biochar amendment is beneficial to the soil-plant system; yet the underlying mechanism is not fully understood. Integrating microfluidics and multi-omics and using wheat as a model plant, we found biochar induces differential root exudates, especially complex molecules like secondary metabolites and signaling cues, and rewires the rhizosphere microbiome, evoking a plant-beneficial rhizosphere microbiome centered by diverse plant growth promoting rhizobacteria (PGPR) known to participate in nitrogen cycling, organic matter turnover, nutrient acquisition, phytohormone metabolism, and stress resistance. Network analysis and machine learning identified high co-occurrence between specific root exudates and PGPR. qPCR, 16S rRNA gene sequencing, and untargeted soil metabolomics suggested the restructured rhizosphere microbiome may have shifted nitrogen and methane metabolism leading to reduced potential of N2O and methane emissions, and may participate in the metabolism of signaling cues and redox reactions. This study provides new insights into biochar's profound impact on the soil-plant system and highlights the potential of engineering the rhizosphere through reshaping root-microbe interactions.

KEYWORDS: *biochar, root exudates, secondary metabolites, rhizosphere microbiome, plant growth promoting rhizobacteria, soil metabolome, nitrogen cycling, methane cycling*

1. INTRODUCTION

Sustainable soil management is vital for safeguarding crop production, environmental health, and human well-being.[1] Biochar has been widely recognized as a multifunctional soil enhancer, capable of improving soil health, boosting crop productivity and stress resistance, reducing nutrient leaching, and mitigating greenhouse gas (GHG) emissions.[2–4] These benefits are often attributed to biochar-induced changes in soil physicochemical properties, such as increased nutrient availability, enhanced water-holding capacity, and reduced acidity or toxic substances.[2] Emerging evidence including our research,[5] however, started to unveil more profound influences of biochar on the soil-plant system.

Soil is a dynamic living system, comprising diverse and complex microbial communities that drive numerous biogeochemical reactions.[6] Increasing evidence suggests that biochar amendment can alter microbial abundance, diversity, community structure, and functional compositions, as synthesized in our meta-analysis.[3,7] However, few studies have investigated biochar's effects on the rhizosphere–a narrow, dynamic zone that serves as a critical interface between plant roots and soil microorganisms and a key component of the plant holobiont.[3,8,9] Our recent study found that biochar can modulate root endometabolites and rhizosphere microbiome.[5] But not all root endometabolites are secreted into the soil; root exudates that are actively secreted directly influence rhizosphere chemistry and thus require further investigation.

Plants use root exudates to recruit plant-growth promoting rhizobacteria (PGPR) and thereby gain growth advantages such as enhanced resistance to diseases and stresses.[8,9] Associations between biochar-induced root exudates and PGPR enrichment is still unknown. Further, nitrogen (N) is a key limiting nutrient for plant productivity in most terrestrial ecosystems, especially croplands.[10,11] While biochar is reported to affect microbially mediated N cycling, including N fixation, nitrification, and denitrification, in bulk soil,[3,12] its effect on rhizosphere N cycling is not well understood. Similarly, biochar's effect on rhizosphere methane cycling is poorly understood. Specifically, the role of biochar-induced root exudates therein is understudied. Unleashing biochar's potential in sustainable crop production requires a mechanistic

61 understanding of biochar's modulating effects on root exudation and the rhizosphere microbiome.

62 This study aimed to use wheat (*Triticum aestivum L.*), a fertilizer-intensive crop, as a model
63 plant to elucidate biochar-induced chemical and biological shifts in the rhizosphere, with a focus
64 on molecular mechanisms of biochar-induced rhizosphere reprogramming. Three specific
65 objectives were: (1) identify biochar-induced root exudates, (2) characterize biochar-induced, root
66 exudate-mediated rhizosphere microbiome restructuring, and (3) determine biochar's modulation
67 on rhizosphere biogeochemistry, especially N and methane cycling. To that end, we conducted
68 controlled experiments using laboratory-produced, well-characterized wheat biochar and a
69 microfluidics device called EcoFAB (ecosystem fabrication), a modular growth system developed
70 for studying the rhizosphere throughout plant development stages.[13] We analyzed root exudates
71 and the soil metabolome using high-resolution mass spectrum (HRMS)-based untargeted
72 metabolomics, the rhizosphere microbiome and its potential function using next-generation
73 sequencing and real-time quantitative PCR (qPCR), and root exudate-microbe associations using
74 a combination of network analysis and machine learning. Our work provides new mechanistic
75 insights into biochar's multifaceted roles in reprogramming the rhizosphere and the potential of
76 engineering the rhizosphere through reshaping root-microbe interactions.

77

78 **2. MATERIALS AND METHODS**

79 **2.1. Biochar production and characterization, and EcoFAB fabrication**

80 Biochar was produced by slow pyrolysis of wheat straw (350 °C for 30 min) in a laboratory
81 reactor, the same as our prior work.[5,14] We chose the pyrolysis temperature due to the fact that
82 biochar produced at lower pyrolysis temperatures tends to promote soil enzyme activity more than
83 biochar produced at higher pyrolysis temperatures.[3] Biochar was characterized using
84 conventional (e.g., pH, N species) and advanced approaches (e.g., Fourier-transform infrared
85 spectroscopy, X-ray diffraction) (details in the Supporting Information (SI)).

86 We used EcoFAB devices, a fabricated ecosystem, for wheat plant cultivation, rhizosphere
87 observation, and sample collection.[13,15] This setting enables continuous investigation of the

88 rhizosphere under highly controlled conditions.[16] We downloaded the original design files
89 (https://eco-fab.org/device-design/) and customized the design to accommodate wheat seedlings.
90 Acrylonitrile butadiene styrene (ABS) mold parts were fabricated using a MakerBot Replicator 2X
91 3D printer, acrylic mold parts were fabricated on a lathe machine, and the assembled mold was
92 used to cast polydimethylsiloxane (PDMS) layers (**Fig 1A**). Our prototype EcoFAB device
93 consisted of a PDMS oval chamber (97.6 × 64 × 3.2 mm) adhering to a large rectangular coverslip
94 (102 × 76 × 1.2 mm) (Ted Pella) in an airtight way (**Fig 1A**). Each device was enclosed in a
95 transparent cover box to maintain a sterile environment for plant experiment (**Fig 1B**). Before
96 experiments, the EcoFAB chamber was rinsed with sterile Milli-Q water; the device surface and
97 the cover box were sterilized using 70% ethanol for 30 minutes and then 100% ethanol for 5 min.
98 More details about EcoFAB fabrication and device assembly are in the SI.
99
100 **2.2. Plant experiment and sample collection**
101 We applied wheat biochar at a rate of 0.25% (w/w) based on cumulative evidence that
102 lower rates promote plant growth while higher rates inhibit growth and our prior observation that
103 wheat biochar at 0.25% rate yields unique rhizosphere alterations.[5] To prepare soil slurries, 100
104 g of agricultural soil (properties in **Table S1**) was added to 1 L sterile Milli-Q water, with or without
105 biochar. Soil slurries were shaken for 16 hours to reach thorough mixing, and slowly injected into
106 each EcoFAB chamber with a sterile syringe. Wheat seeds were germinated and seedlings of
107 similar sizes were transferred aseptically into sterilized EcoFAB devices containing soil slurries
108 with or without biochar (one plant per device; four biological replicates for each treatment) (**Fig**
109 **1B**). Plants were cultivated under full spectrum LED light simulating natural sunlight (12 hour light,
110 12 hour dark) and controlled humidity (80%) at 25 °C for 21 days, and the development of root
111 systems was monitored (**Fig 1B**). Milli-Q water was added to EcoFAB devices every three days
112 to maintain humidity. To ensure reproducibility, the experiment was conducted twice.
113 After 21 days, individual EcoFAB devices were dissembled, and remaining soil slurries
114 and plants were collected (sequential sample collections shown in **Fig 1C**). Soil slurries were

115 immediately stored at -80°C until metabolite extraction, while plants were immediately processed
116 to collect ectorhizosphere soils like in our prior studies.[5,17] After ectorhizosphere soil removal,
117 individual plants with clean root surfaces were transferred to sterile 15 mL centrifuge tubes
118 containing 15 mL Milli-Q water to allow for exudation for 24 hours like in our prior study.[18] An
119 aliquot of the collected exudated solution (1.5 mL) was transferred to a 2.0 mL sterile
120 microcentrifuge tube, dried using a vacuum concentrator (Savant SpeedVac SPD300DDA,
121 Thermo Scientific), and 1.5 mL of methanol solution (80% v/v in Milli-Q water) was added to the
122 tube, followed by vortexing for 15 minutes and sonication bath for 5 minutes at room temperature.
123 The resulting extract was filtered through a 0.22 μm PVDF filter (Millipore) and stored at -80 °C
124 until metabolomics analysis. Similar procedures were used to extract soil exometabolites (detailed
125 in the SI).
126
127 **2.3. Untargeted metabolomics using HRMS**
128 Root exudates and soil exometabolites were analyzed using liquid chromatography- mass
129 spectrometry (LC-MS) performed on a Vanquish LC system in conjunction with a Q Exactive HF
130 Orbitrap MS coupled with an electrospray ionization (ESI) source (Thermo Fisher). The MS has
131 a resolving power of up to 240,000 FWHM (Full Width at Half Maximum) at 500 m/z and a mass
132 range of 20-1200 m/z. Extract aliquots of 10 μL were injected into a Hypersil GOLD C18 column
133 (1.9 μm, 2.1×150 mm) (Thermo Fisher) operated at 30 °C. LC mobile phases consisted of solvent
134 A (0.1% formic acid in Milli-Q water) and solvent B (0.1% formic acid in LC/MS grade acetonitrile),
135 and the flow rate was maintained at 300 μL/min. MS was operated in both positive and negative
136 ion mode (ESI+ and ESI-). More LC-MS details are in the SI. Spectral data was processed as
137 before.[5] Raw data was converted to the generic mzXML format and processed using three
138 platforms (MetaboAnalyst 6.0, XCMS, MZmine3).[19–21] The resulting feature tables were merged
139 without redundancy and further processed in MetaboAnalyst 6.0 for functional analysis.
140 Compounds were converted to the International Union of Pure and Applied Chemistry (IUPAC)
141 names and classified to the “Class” level of the purely structure-based chemical taxonomy

142 (ChemOnt) using ClassyFire.[22] Significant fold change (FC) was determined by the Mann-Whitney
143 *U* test with Benjamini-Hochberg correction ($|\log_2 FC| > 1$ and $p < 0.05$). Principal coordinates
144 analysis and network analysis are detailed in the SI.
145
146 **2.4. Next generation sequencing, qPCR, and biofilm assay**
147 Metagenomic DNA was extracted from rhizosphere soils using the ZymoBIOMICS
148 DNA/RNA Miniprep Kit following the manufacturer's protocol (Zymo Research). A PowerLyzer
149 Homogenizer was used to maximize extraction efficiency. The resulting DNA was assessed on a
150 Qubit 4 fluorometer with the 1× dsDNA High Sensitivity Assay Kit (Thermo Fisher) and by
151 electrophoresis. 16S rRNA gene sequencing and data processing (QIIME2, DADA2, phyloseq)
152 were performed as before.[5,23–25] The "edgeR" package was used to identify differential taxa
153 between samples. PICRUSt2 was used to infer metagenomic functional contents; PICRUSt2
154 predictions were subjected to differential abundance analysis using the R package
155 "ggpicrust2".[26,27] Microbial community growth rate, i.e., median predicted minimum doubling time
156 (mPMDT), was predicted using the R package "gRodon".[28,29] Microbial network analysis was
157 constructed using SparCC.[30] Community assembly mechanisms were assessed using the null
158 model approach. We calculated the β-nearest taxon index (βNTI) using the R package "iCAMP"
159 to estimate the relative importance of deterministic versus stochastic assembly processes,[31] and
160 calculated the Raup-Crick metric using Bray-Curtis dissimilarities (RC_{BC}) to estimate the relative
161 importance of selection, drift, dispersal limitation, and homogenizing dispersion.[32] More details on
162 sequencing and data processing are in the SI.
163 While PICRUSt2 inference provides a more comprehensive snapshot of a community's
164 potential function, inference accuracy varies. Therefore, we used qPCR to quantify the abundance
165 of eubacterial 16S rRNA gene (proxy of total bacteria) and key genes involved in nitrogen (*nifH*,
166 *nxrA*, *nirK*, *nirS*, *nosZ* Clade I) and methane (*mcrA*, *pmoA*) cycling using established primers
167 (**Table S2**). qPCR was performed on a CFX Duet Real-Time PCR System (BioRad) with
168 SsoAdvanced universal SYBR green supermix (Bio-Rad), 2 µL of DNA template (2-fold diluted to

169 mitigate soil matrix inhibition effect), and primers (0.48 μM each) in a 25 μL reaction volume
170 (details in the SI).
171 To test whether biochar-induced root exudates promote biofilm formation compared to root
172 exudates from control plants, we conducted a biofilm assay using a model soil bacterium
173 *Pseudomonas putida* KT2440. The results were normalized against dissolved organic carbon
174 (DOC) content in root exudates to exclude the effect of varying carbon content (details in the SI).
175
176 **2.5. Multi-omics integration**
177 We used two approaches to identify associations between root exudates and rhizosphere
178 microbes: (1) OmicsNet 2.0 which utilizes multiple databases to create multi-omics networks, and
179 (2) mmvec (microbe-metabolite vectors), a neural network approach that predicts an entire
180 metabolite profile from a single microbe sequence.[33,34] OmicsNet 2.0 calculates metabolite-
181 microbe correlations based on microbial metabolic capacity and pertinent proteins that are
182 predicted using high-quality genome-scale metabolic models. The mmvec approach estimates
183 the conditional probability of observing a metabolite given that a microbe is present to identify the
184 most likely metabolite-microbe interactions. Compared to approaches based on correlation (e.g.,
185 Spearman's) or network (e.g., SparCC), mmvec can identify previously undiscovered patterns
186 and is less prone to false discovery (positive or negative) as it provides consistency between
187 absolute and relative abundances of compositional data. However, mmvec does not calculate the
188 statistical significance or confidence interval of each metabolite-microbe pair. Here we combined
189 the two approaches to maximize the discovery of true metabolite-microbe interactions. Similar
190 approaches were used to identify and visualize associations between rhizosphere microbes and
191 soil exometabolites. More details are in the SI.
192
193 **2.6. General statistics and data visualization**
194 Bioinformatics, statistics, and data visualization were performed in R (4.2.1) and Python
195 (3.7) with various R packages and Python modules. Significant differences were determined using

196 one-way analysis of variance (ANOVA) or Welch's *t* test, nonparametric statistics (Wilcoxon or
197 Kruskal-Wallis), and permutational multivariate analysis of variance (PERMANOVA), depending
198 on the variable. Network visualization used Gephi (0.10.1) and Cytoscape (3.9.1). More details
199 are in the SI.
200

201 **3. RESULTS AND DISCUSSION**

202 **3.1. Biochar significantly promotes plant growth**

203 SEM indicated the wheat biochar used here had a porous morphology (**Fig 2A**). FTIR
204 spectra showed the biochar contained aromatic compounds (particularly those with benzene rings
205 and quinone groups), C–O bonds from esters or ethers, nitriles, silicates and/or carbonates, and
206 possibly C–N or P–O (**Fig 2B; Fig S2**) (more in the SI).[35,36] EDS analysis revealed the surface of
207 the biochar predominantly contained C (62.36%), O (24.52%), Si (6.13%), K (3.06%), and Ca
208 (1.04%) (averaged atomic%, n = 29) (**Fig 2C**). Consistent with the EDS results, XRD spectra
209 indicated the presence of amorphous C, graphite, and various mineral crystals containing Si, K,
210 and Ca (**Fig 2D**) (more in the SI).[36,37] These results reflect the biochar's feedstock (wheat straw)
211 and the production condition (slow pyrolysis at 350 °C).

212 In the 21-day EcoFAB experiment, application of 0.25% (w/w) wheat biochar yielded 1.59
213 times more fresh weight of shoots (Welch *t* test: $p < 0.001$) (**Fig S3**). Fresh weight of roots had
214 no significant difference (Welch *t* test: $p = 0.413$), but biochar-treated plants had more lateral roots
215 (**Fig S3**). These results are consistent with our prior 15-day pot study and suggest biochar's plant
216 growth promotion effect may be scalable.[5]
217

218 **3.2. Biochar induces differential root exudation**

219 Biochar induced differential root exudation (**Table S3**), systematically regulating root
220 metabolism, as evidenced by increased average degree and centrality of root exudate co-
221 occurrence network (**Fig 3A**). Specifically, biochar significantly regulates carbohydrate
222 metabolism, glycan biosynthesis, the metabolism of terpenoids and polyketides, and nucleotide

223 metabolism, all of which are highly involved in plant growth and development, signaling, and
224 stress defense.[2,3]

225 Among the 312 compounds detected across samples, six were only identified in biochar-
226 induced root exudates, including two flavanonols, one flavanone and its direct precursor, a
227 phenolic ester, and dUMP (**Table S3**). Further, biochar significantly affected 39 compounds from
228 14 ChemOnt classes ($|Log_2FC| > 1$, *p-adjusted* < 0.05): 10 organooxygen compounds, 6
229 flavonoids, 3 prenol lipids, 3 fatty acyls, 2 from each of four classes (organonitrogen compounds,
230 steroids and steroid derivatives, imidazopyrimidines, carboxylic acids and derivatives), 1 from
231 each of five classes (5'-deoxyribonucleosides, pyrimidine nucleotides, furanoid lignans, linear 1,3-
232 diarylpropanoids, organic phosphoric acids and derivatives), and 4 unclassed chemicals (**Fig 3B**).
233 Two compounds having regulatory roles in plant defense were upregulated, including (22S)-22-
234 hydroxycampest-4-en-3-one (a direct precursor of brassinosteroids (BRs)) (2.6 fold) and 2,4-
235 dihydroxy-1,4-benzoxazin-3-one-glucoside (DIBOA-Glc, a benzoxazinoid (BX) compound) (5.2
236 fold). BRs are phytohormones indispensable for root growth and BR biosynthesis is largely
237 restricted to the root elongation zone.[38] DIBOA-Glc is the glycosylation product of DIBOA, the
238 most abundant BX in cereal crops, and the precursor of defense-active compound DIMBOA-Glc.[39]
239 BX glucosides are stored in vacuoles and released over time to the rhizosphere where their
240 derivatives can suppress weeds and hostile microbes while enriching beneficial microbes.[40,41]
241 These results indicate that biochar may promote plant growth by upregulating root exudates that
242 have antimicrobial and antioxidant activities. Further, BRs and BXs are secondary metabolites
243 known for their signaling functions, and increasing evidence reveals they also mediate plant-
244 microbe interactions such that shifts in their biosynthesis can reshape the rhizosphere
245 microbiome.[40–44] Here, by upregulating biosynthesis of plant signaling metabolites, biochar may
246 modulate the rhizosphere microbiome, which indeed occurred as discussed later. Thirty-six root
247 exudates were downregulated, including six flavonoids. Flavonoids are essential in plant fitness
248 and rhizosphere microbiome assembly.[45] Downregulation of flavonoid biosynthesis could reflect
249 either reduced stress due to scavenging of reactive oxygen species or BR-induced inhibition of

250 flavonoid biosynthesis.[46] It may also reflect shifted flavonoid biosynthesis as several flavonoids,
251 including 2 flavanonols (dihydrokaempferol, (+)-2,3-dihydrofisetin), one flavanone and its direct
252 precursor (eriodictyol and eriodictyol chalcone), and a phenolic ester (4-coumaroylshikimate)
253 were only detected in biochar-treated root exudates. Overall, our results provide new chemical
254 insights into widely observed biochar benefits on crop productivity.[47]

255 A majority (81.4%) of the 312 exudate compounds were previously detected inside of root
256 tissues (**Fig S5**; the SI text).[5] But 58 exudate compounds were not previously detected within
257 roots, including 8 fatty acyls, 6 organooxygen compounds, 5 pyrimidine nucleotides, 5 purine
258 nucleotides, 4 carboxylic acids and derivatives, 3 flavonoids, 1 isoflavonoid, 3 prenol lipids, among
259 others, such as DIBOA-Glc and gibberellin A29-catabolite (GA29-catabolite, a deactivated
260 catabolite from GA20) (**Fig S5; Table S4**). These 58 actively exudated compounds have critical
261 roles in the rhizosphere: Fatty acyls and prenol lipids, organooxygen compounds, carboxylic acids
262 and derivatives, and flavonoids and isoflavonoids are involved in rhizosphere signaling, able to
263 mediate plant root-microbe interactions.[9,45,48] Among the detected fatty acyls, linolenic acids are
264 plant defense signaling molecules;[49] 2'-deoxymugineic acid is an iron (III) phytosiderophore,
265 influencing rhizosphere microbiome composition through iron competition.[8,50] Five of the six
266 detected organooxygen compounds were inositol phosphates, a major pool of organic
267 phosphorus in soil and signaling molecules mediating microbial root colonization.[51] These results,
268 along with our prior pot study,[5] suggest biochar-induced metabolic alterations in roots and
269 subsequent exudation of exudates that may modulate plant-microbe interactions.

270

271 **3.3. Rhizosphere microbiome restructuring and its association with biochar-induced root**
272 **exudates**

273 ***3.3.1. Biochar rewires the rhizosphere microbiome and microbial interactions***

274 In the native wheat rhizosphere, the top 10 phyla and top 40 genera comprised 60% and
275 35% of all prokaryotes, respectively, reflecting the core rhizosphere microbiome of plant,
276 especially cereals.[8] Biochar had limited influence on rhizosphere microbial alpha diversity but

277 considerably altered microbiome composition (PERMANOVA test: $p = 0.001$ for round × treatment)
278 (**Fig 4A-B**), promoting 12 genera while suppressing 9 genera (**Fig S6-S7; Table S5**) (more in the
279 SI).

280 Remarkably, biochar enhanced microbial interactions, evidenced by greater microbial
281 network modularity and centrality and a large number of newly emerged keystone genera (60 vs.
282 53 in the treated vs. native rhizosphere) (**Fig 4C; Fig S8; Table S6-S8**). Twelve common keystone
283 bacterial genera were observed in the native and treated rhizosphere, including nine PGPR from
284 Actinobacteria, Alphaproteobacteria and Gammaproteobacteria: *Bradyrhizobium* and *Microvirga*
285 are N-fixing bacteria;[52] *Paracoccus* can metabolize nitrogen, nitrate, and ammonia;[53] *Lysobacter*
286 and *Stenotrophomonas* can suppress soil-borne pathogens by producing lytic or antimicrobial
287 substances;[54,55] *Shinella* can degrade polycyclic aromatic hydrocarbons;[56] *Cellvibrio* has an
288 extensive repertoire of carbohydrate-active enzymes for degrading polysaccharides (cellulose,
289 dextran, xylan, chitin, and starch), thus enhancing organic matter turnover;[57] *Rhodococcus*
290 contributes to N cycling and influences plant stress response and growth by metabolizing the
291 phytohormone abscisic acid (ABA) and producing the phytohormone indole-3-acetic acid
292 (IAA);[58,59] *Solirubrobacter* can produce IAA and improve nutrient bioavailability through
293 assimilatory reduction of sulphate and utilizing a wide range of carbohydrates (more in the SI).[60]

294 Besides these common keystone genera, the native rhizosphere microbiome had classic
295 rhizosphere keystone genera, such as those able to degrade plant cell wall polysaccharides
296 (detailed in the SI), whereas the biochar-treated rhizosphere had additional diverse PGPR as
297 keystone genera (**Fig 4C**). These included *Chryseobacterium* (with greatest betweenness and
298 closeness centrality) that can enhance plant nutrient acquisition, degrade aromatic compounds,
299 produce antioxidant enzymes, synthesize IAA, and lower plant stress levels by reducing the
300 immediate precursor of the stress phytohormone ethylene using 1-aminocyclopropane-1-
301 carboxylate (ACC) deaminase.[9,61] Another example was methylotrophic
302 *Methylobacterium*/*Methylorubrum* (connector hub) that can synthesize developmental
303 phytohormones (auxins, gibberellins, cytokinins) and ACC deaminase and fix nitrogen.[9,62] Other

304 newly emerged keystone PGPR genera in the biochar-treated rhizosphere included N-fixers
305 *Allorhizobium-Neorhizobium-Pararhizobium-Rhizobium* and *Azospirillaceae*,[40] denitrifiers
306 *Magnetospirillum*,[63] IAA-producing *Nocardia*,[64] Planctomycetes *OM190* (module hub) able to
307 produce diverse secondary metabolites including antimicrobial compounds,[65] and *Solibacillus* that
308 can produce IAA and plant singling molecule hydrogen cyanide and secrete siderophores to
309 solubilize or chelate minerals.[66]

310 These results suggest a potential microbial mechanism for the widely reported but poorly
311 understood plant-promoting effect of biochar: It elicits diverse PGPR, including nitrogen fixers,
312 denitrifiers, and phytohormone producers, to emerge as keystone taxa. Therefore, the biochar-
313 treated rhizosphere microbiome may grant the plant with multiple benefits.[67] Indeed, biochar-
314 treated plants had higher shoot mass and more lateral roots (Section 3.1), a phenomenon likely
315 attributed to the enrichment of PGPR and the upregulation of BR biosynthesis (Section 3.2). Given
316 the significance of keystone taxa in overall microbiome structure and functioning,[8] future research
317 would benefit from directly characterizing functions of the keystone microbes in the biochar-
318 treated rhizosphere.

319

320 ***3.3.2. Rhizosphere microbiome rewiring is associated with biochar-induced root exudates***

321 Plants use root exudates to recruit and tune the rhizosphere microbiome.[8] Since biochar
322 induced differential exudation, particularly polyphenols and lipids, we hypothesized that shifts in
323 root exudate chemistry may be associated with rhizosphere microbiome restructuring, selectively
324 enriching or suppressing bacterial taxa, through metabolic coupling of biochar-induced root
325 exudates with microbial substrate-use preferences as suggested by recent evidence from
326 laboratory experiments and genome-informed modeling.[68–70] In line with this hypothesis,
327 computational prediction showed the biochar-rewired rhizosphere microbial community had a
328 slower growth rate than the native microbiome (**Fig 4D**), likely due to a switch from higher growth
329 and lower substrate utilization efficiency to lower growth and higher substrate utilization
330 efficiency.[68,70] To validate this genome-informed, community-level prediction, we tested biofilm

331 formation of a model soil bacterium *P. putida* KT2440 under exposure to control or biochar-
332 induced root exudates (**Fig S9A**). While root exudates from control and biochar-treated plants
333 had similar levels of DOC (**Fig S9C**) (p = 0.607), biochar-induced root exudates resulted in less
334 *P. putida* biofilm within 48 hours (**Fig S9B**) (p = 0.004), consistent with the computational
335 prediction that biochar-induced root exudates favor slow-growing microbes capable of utilizing
336 complex molecules. It should be noted that this shift did not significantly change the total bacteria
337 number. Instead, biochar insignificantly increased the number of rhizosphere bacteria as shown
338 by qPCR results (**Fig S10**). Analysis of community assembly mechanisms found that dispersal
339 limitation dominated rhizosphere community turnover (**Fig S11A-B**), suggesting low dispersal
340 rates in the rhizosphere niche where weak or unstructured selective pressures from substrate
341 utilization enable high compositional turnover.[31] Together, computational prediction, biofilm assay,
342 and community assembly analysis support our hypothesis that biochar rewired the rhizosphere
343 microbiome through metabolic coupling of biochar-induced root exudates with microbial
344 substrate-use preferences.

345 Our hypothesis is further supported by the coincidence of biochar-upregulated root
346 exudates like DIBOA-Glc and biochar-enriched bacteria having BXs-enhanced growth (detailed
347 in the SI). This motivated us to explore specific microbe-exudate compound associations.
348 Combining the co-occurrence network (OmicsNet 2.0) and neural network (mmvec) approaches,
349 we identified 12 bacterial genera, including 11 PGPR (*Bacillus*, *Blastococcus*, *Bradyrhizobium*,
350 *Brevundimonas*, *Mesorhizobium*, *Nevskia*, *Paenibacillus*, *Pantoea*, *Pseudomonas*, *Rhodococcus*,
351 *Roseomonas*),[52] with highest associations with biochar-induced root exudates (mainly plant
352 secondary metabolites) (**Fig 5**). Extremely high co-occurrence probability may manifest when a
353 compound is a preferred substrate to certain bacteria,[40,68–70] and the root exudate-microbe
354 associations observed here are in line with existing literature.

355 Here four flavonols, including three quercetin derivatives and one kaempferol derivative,
356 had varying co-occurrence with the 12 bacterial genera: Isoquercitrin (quercetin 3-O-glucoside)
357 had very high co-occurrence with all the 12 genera, particularly *Pantoea*; quercetin 3-O-

358 rhamnoside-7-O-glucoside and kaempferol-3-O-rhamnoside had similar co-occurrence patterns
359 with several microbes, opposite to quercitrin (quercetin 3-O-rhamnoside) (**Fig 5**). Quercetin and
360 its derivatives can stimulate PGPR, including *Pantoea* that harbors quercetin dioxygenases for
361 degrading flavonols.[45,71] This aligns with our observation of very high co-occurrence probabilities
362 between *Pantoea* and two quercetin derivatives (quercitrin > isoquercitrin). Three GAs, GA12-
363 aldehyde (early precursor of bioactive GAs), GA44 open lactone (key intermediate in bioactive
364 GA1 synthesis), and GA34-catabolite (deactivated catabolite from bioactive GA4), had varying
365 co-occurrence with all the 12 bacterial genera, with GA44 open lactone and GA34-catabolite
366 showing opposite patterns. GA phytohormones are crucial for many aspects of plant growth and
367 development. Appropriate levels of bioactive GAs are tightly regulated in plants and also
368 modulated by PGPR such as *Bacillus*, *Bradyrhizobium*, and *Mesorhizobium* that possess GA
369 metabolic pathways.[72–74] Here *Bacillus* co-occurred with GA34-catabolite, while *Bradyrhizobium*
370 and *Mesorhizobium* had very high co-occurrence probability with GA44 open lactone and GA34-
371 catabolite, respectively. (S)-Abscisic acid, the naturally occurring and bioactive form of
372 phytohormone ABA, and its direct catabolite 8'-hydroxyabscisic acid had high co-occurrence with
373 *Blastococcus*, *Bradyrhizobium*, and *Roseomonas*, suggesting their participation in ABA
374 metabolism. Indeed, PGPR like *Bradyrhizobium* can regulate ABA levels in the rhizosphere
375 through biosynthesis and catabolism of ABA.[41,72] Two glycosides of phytohormone cytokinins, cis-
376 zeatin-O-glucoside and dihydrozeatin-O-glucoside, had opposite associations with several PGPR,
377 with cis-zeatin-O-glucoside showing very high co-occurrence with four PGPR (*Mesorhizobium* >
378 *Rhodococcus* > *Pseudomonas* > *Bacillus*). Among these PGPR, *Rhodococcus* and
379 *Pseudomonas* are known to produce cytokinins.[72,75]

380 Taken together, our analyses of hypothetical community growth rate, biofilm formation
381 tendency, community assembly mechanism, and specific microbe-exudate associations suggest
382 that biochar-induced root exudates may play a key role in the rhizosphere microbiome
383 restructuring. In particular, secondary metabolites such as flavonoids (flavonols) and
384 developmental phytohormones (GAs, ABA, cytokinins) may evoke diverse PGPR capable of

385 utilizing these compounds. While biochar-induced microbiome shifts in bulk soil has been well
386 documented (e.g., our meta-analysis[3]), this study suggests additional modulation mechanisms in
387 the rhizosphere through metabolic coupling of root exudates with microbial substrate-use
388 preferences. Future research employing metagenomics and metatranscriptomics, as well as
389 using pure PGPR cultures, is required to ascertain our observations and elaborate underlying
390 biochemical mechanisms.
391
392 **3.4. Biochar-treated rhizosphere microbiome has shifted functions**
393 ***3.4.1. Shifted nitrogen and methane cycling***
394 Many studies have reported biochar's impact on N and methane cycling in bulk soil,
395 partially due to changes in microbial communities.[2,3] We hypothesized such effects also occur in
396 the rhizosphere with additional influences from root exudates. Our qPCR measurements found
397 increased abundance of *nifH* (N fixation), *nxrA* (nitrification, NO_2^- to NO_3^-), *nirS* (denitrification,
398 NO_2^- to NO) and *nosZ* (denitrification, N_2O to N_2), and reduced abundance of *nirK* (denitrification,
399 NO_2^- to NO) in the biochar-treated rhizosphere, although the differences were insignificant (**Fig**
400 **6B**). These trends are consistent with the emergence of N-fixing bacteria (e.g., *Allorhizobium-*
401 *Neorhizobium-Pararhizobium-Rhizobium*, *Azospirillaceae*) as keystone taxa and the enrichment
402 of ammonia-oxidizing bacteria (e.g., *Nitrosomonas*) in the biochar-treated rhizosphere (**Fig 4C**;
403 **Table S5**). Interestingly, biochar-induced increase in *nxrA* abundance coincided with a drastic
404 enrichment of *Roseomonas*, a genus known to harbor *nxrA*,[76] and showed high co-occurrence
405 with biochar-induced ABA (a terpenoid phytohormone) and its direct catabolite 8'-hydroxyabscisic
406 acid (**Fig 5**). In complete denitrification, NO_2^- is reduced to NO by nitrite reductases (*nirK* and
407 *nirS*), while NO is further reduced to N_2O by nitric oxide reductases (*nor*) and N_2O reduced to N_2
408 by nitrous oxide reductase (*nosZ*). Changes in the relative abundance of these genes are
409 associated with the net emission of N_2O. Specifically, the (*nirK*+*nirS*)/*nosZ* ratio has been used to
410 estimate N_2O emission potential.[77] Our qPCR results showed a reduced (*nirK*+*nirS*)/*nosZ* ratio in
411 the biochar-treated rhizosphere, suggesting a promotion of complete denitrification and a

412 reduction of N_2O emission potential, likely due to biochar's role in facilitating electron transfer to
413 denitrifying microbes.[78] qPCR results also showed a reduction in the (*nirK*/*nirS*) ratio, suggesting
414 a shift from *nirK*-type nitrifiers, which often lack the *nosZ* gene, to *nirS*-type nitrifiers.[79] This
415 observation is consistent with the emergence of *Magnetospirillum* as keystone taxa and the
416 enrichment of *Sporomusa* in the biochar-treated rhizosphere (**Fig 4C**; **Table S5**).
417 *Magnetospirillum* harbors a complete denitrification pathway, able to reduce NO_3^- to N_2.[80] It should
418 be noted that certain *Sporomusa* species contain a recently-characterized novel lactonase-type
419 N_2O reductase that cannot be captured by existing primers including those used here.[81] Overall,
420 these results suggest that biochar may promote nitrogen fixation and nitrification while reducing
421 N_2O emission potential in the rhizosphere through restructuring the rhizosphere microbiome.

422 qPCR did not detect *mcrA* encoding the methyl-coenzyme M (CoM) reductase complex in
423 any sample, reflecting a low representation of *mcrA*-containing methanogens in the
424 ectorhizosphere. Consistently, PICRUSt2 predicted that biochar suppressed CoM biosynthesis I,
425 which is required to produce methyl-CoM (**Fig 6A**).[82] qPCR found increased *pmoA* (encoding
426 membrane-bound particulate methane monooxygenase[83]) in the biochar-treated rhizosphere,
427 suggesting enhanced methane oxidation although the differences were insignificant (**Fig 6B**).
428 Consistently, two C5 prenol lipids, isopentenyl pyrophosphate and dimethylallylpyrophosphate,
429 were only detected in the biochar-treated soil metabolome (**Fig 6C; Table S12**). These prenol
430 lipids are building blocks of all isoprenoids, including bacteriohopanepolyols that are crucial
431 structural components of methanotroph membranes. Their detection in the biochar-treated soil
432 metabolome may suggest stimulated growth and subsequent lysis of methanotrophs. Further,
433 biochar may have influenced methylated substrates and thereby methylotrophic
434 methanogenesis,[84] as suggested by PICRUSt2-predicted enrichment (>1000 fold) of methionine
435 salvage pathway (MSP) in the biochar-treated rhizosphere (**Fig 6A**) and the detection of several
436 MPS intermediates in root exudates and the soil metabolome, as well as high co-occurrence of
437 specific PGPR and a methylthio compound downstream in MSP (detailed in the SI). MSP
438 produces methanethiol, a methylated substrate for methylotrophic methanogenesis; both

439 methanethiol methylation and methionine also influence dimethylsulfide, another methylated
440 substrate for methylotrophic methanogenesis.[84,85] However, this hypothesis remains to be verified
441 by metagenomic and metatranscriptomic analysis. The importance of methylotrophic
442 methanogenesis in agricultural methane emissions has only recently been recognized.[86,87] Given
443 the large suite of methylated substrates in root exudates that may be utilized by methylotrophic
444 methanogens and biochar's impact on the chemistry of root exudates, more experimental and
445 field research is needed in this direction.

446 Together, our results from qPCR, function prediction, and untargeted soil metabolomics
447 suggest that in the rhizosphere, biochar-induced microbiome restructuring may lead to shifts in N
448 and methane cycling, resulting in attenuated GHG emissions. Our results also highlight an urgent
449 need of scrutinizing how biochar-induced changes in root exudate chemistry may affect
450 methylotrophic methanogenesis.

451

452 ***3.4.2. Broader changes in rhizosphere microbiome functions***

453 A total of 506 exometabolites were detected in rhizosphere soils (**Fig 7A**). Biochar
454 significantly influenced the soil metabolome chemistry (PERMANOVA: p = 0.04 for treatment)
455 (**Fig 7B**), reflected by 64 most discriminative compounds from 14 ChemOnt classes ($|Log_2FC| >$
456 1, *p-adjusted* < 0.05) (**Fig 6C**) (details in the SI). Remarkably, several plant defense compounds
457 were only detected in the biochar-treated rhizosphere, including lotaustralin and methionine-
458 derived methylthioalkylmalates that are important precursors of sulfur-containing glucosinolates
459 (**Fig 6C; Table S12**).[41] Further, IAA and an indole derivative (5-hydroxyindoleacetaldehyde) were
460 detected in the control rhizosphere but absent in the biochar-treated rhizosphere where 5-
461 hydroxyindoleacetic acid, a direct oxidation product of 5-hydroxyindoleacetaldehyde was
462 detected (**Fig 6C; Table S3; Table S12**). This may suggest microbial metabolism of IAA and is
463 consistent with the enrichment of IAA-producing PGPR (Section 3.3.1).

464 Among the 506 exometabolites, 180 compounds were detected in root exudates collected
465 by hydroponic secretion, while 326 compounds were only found in the soil metabolome (**Fig 7A;**

466 **Table S12**). The 326 exometabolites consisted of compounds secreted by roots in contact with
467 rhizosphere microbes, as well as microbial metabolites. DIBOA-Glc was only detected in
468 hydroponic secretion (**Fig 2B**), while its active form DIBOA was only detected in soil
469 exometabolites and had high co-occurrence probability with 7 PGPR (**Fig S14**), suggesting BXs
470 may be used as signaling cues for recruiting PGPR.[40,75] Various GAs were detected in both root
471 exudates and soil exometabolites, but an early precursor of bioactive GAs (GA12-aldehyde) was
472 only detected in root exudates, whereas two GA catabolites (GA8, GA8-catabolite) and one
473 intermediate (GA24) were only detected in the soil metabolome (**Table S12**), with GA24 showing
474 high co-occurrence probability with several PGPR (**Fig S14**), especially *Bradyrhizobium* that is
475 known to possess GA metabolic pathways.[72–74]

476 After mapping the 326 soil exometabolites to predicted microbial pathways (**Table S13**)
477 and comparing microbe-root exudate and microbe-exometabolite co-occurrence networks (**Table**
478 **S9**), we found biochar likely influenced microbial synthesis of three vitamins (biotin, phylloquinone,
479 menaquinol) (more details in the SI). Menaquinone is a vitamin (K12) produced by bacteria and
480 some archaea. Here, the menaquinol percussor 2-succinyl-5-enolpyruvyl-6-hydroxy-3-
481 cyclohexene-1-carboxylic acid was only detected in root exudates, while two immediate
482 metabolites of menaquinone biosynthesis, (1R,6R)-6-hydroxy-2-succinylcyclohexa-2,4-diene-1-
483 carboxylate and 2-succinylbenzoate, were only detected in the soil metabolome (**Table S3; Table**
484 **S12**). Biochar significantly reduced the two intermediates (**Fig 6C**). Coincidentally, PICRUSt2
485 predicted that biochar increased all but one menaquinone biosynthesis genes; meanwhile,
486 menaquinol, the bioactive reduced form of menaquinone, was detected in the soil metabolome
487 (**Fig S15**). These results may suggest biochar-induced boost in microbes that use cellular
488 menaquinone pool for respiratory electron transfer.[88,89] Whether or not these microbes contribute
489 to more complete denitrification, as well as other redox reactions, remains to be investigated.

490 Collectively, our results from untargeted soil metabolomics and function prediction suggest
491 profound modulating effects of biochar on rhizosphere microbiome functionality, ranging from
492 phytohormone metabolism by PGPR to biosynthesis of redox-active quinone compounds. These

493 changes could have significant implications for plant growth and soil biogeochemistry. Future
494 research should integrate metagenomic, metatranscriptomic, and metabolomic data to validate
495 our observations and elaborate underlying microbial mechanisms.
496
497 **3.5. Implications for sustainable crop production and future needs**
498 Rhizosphere engineering has attracted increasing interest as a promising approach for
499 sustainable crop production.[90] Extending from our prior work on metabolites within root tissues,[5]
500 this study is among the first that elaborates biochar-induced systematic shifts in secreted root
501 exudates, the rhizosphere microbiome, and the soil metabolome. Our results suggest new
502 chemical and microbial mechanisms behind the widely reported but poorly understood effects of
503 biochar on the soil-plant system. Specifically, biochar evokes a plant-beneficial rhizosphere
504 microbiome centered by diverse PGPR, and such microbiome restructuring may partially be
505 attributed to biochar-induced changes in root exudate chemistry, particularly complex molecules
506 including a wide range of plant secondary metabolites. Therefore, compared to its modulating
507 effect on the bulk soil microbiome, biochar also modulates the rhizosphere microbiome indirectly
508 through altering rhizosphere chemistry. The restructured rhizosphere microbiome shows
509 alterations in N and methane cycling that may lead to reduced potential of N_2O and CH_4 emissions.
510 Additionally, the restructured microbiome is likely involved in the transformation of signaling cues
511 and a variety of redox reactions, thus having broader implications for the soil-plant system.
512 Several limitations of this study should also be noted. First, the EcoFAB device and the
513 cultivation condition simplify the complexity of the soil-plant system in root exudate chemistry,
514 rhizosphere microbiome diversity, and root-microbe interactions. Future research should leverage
515 larger-scale laboratory experiments and field studies and use other plant models to validate and
516 extend findings from this study. Second, we identified potential associations between specific root
517 exudate compounds and PGPR using a combination of network analysis and machine learning.
518 These associations and the underlying biochemical mechanism should be ascertained by
519 integrated metagenomic/metatranscriptomic analysis and in experiments using model bacterial

520 strains. Third, we used 16S rRNA gene sequencing-based function prediction coupled with
521 untargeted soil metabolomics to infer microbiome functions. Integrating metagenomic,
522 metatranscriptomic, and metabolomic data will provide more conclusive evidence for biochar-
523 induced community-level functional shifts and the links to biochar-induced changes in root
524 exudate chemistry. Nevertheless, this research provides new insights into biochar's multifaceted
525 roles in reprogramming the rhizosphere and highlights the potential of engineering the
526 rhizosphere through reshaping root-microbe interactions using designed biochar or root exudate
527 cocktails. Further, the use of crop residue-derived biochar also exemplifies a circular economy
528 approach valorizing agricultural wastes.[91]
529

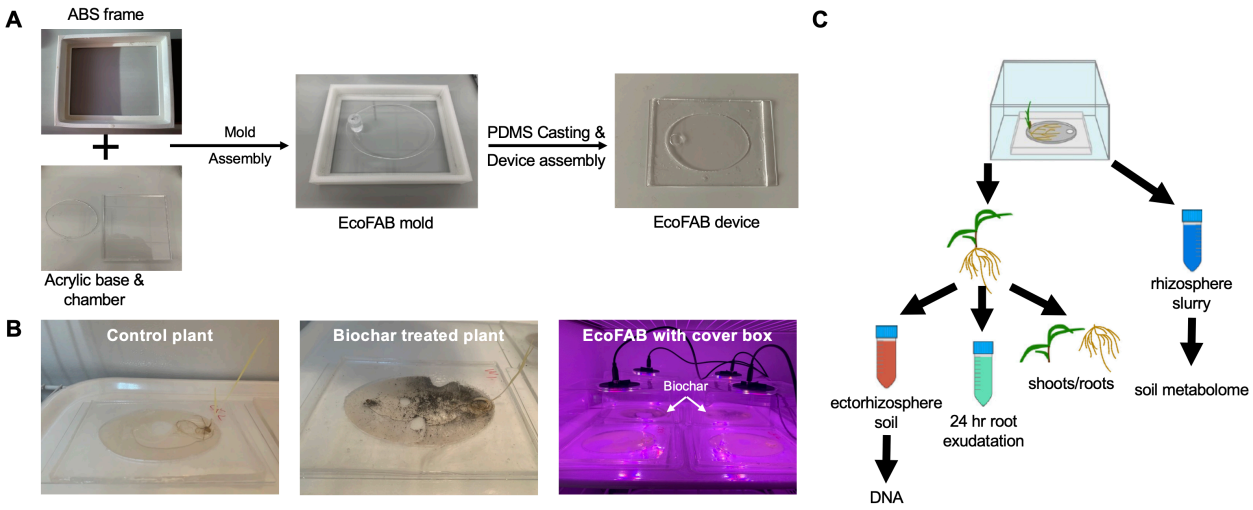

Fig 1. (A) Fabrication of a prototype EcoFAB device. (B) EcoFAB experiment under a sterile and highly controlled environment. The EcoFAB chamber hosted the root system while the plant shoot was covered by a sterile cover box equipped with a LED (full spectrum) control and a humidity monitor. Each EcoFAB device represents a biological replicate, and an individual wheat seedling was cultivated with or without 0.25% (w/w) wheat biochar. (C) Sequential sample collections: (1) rhizosphere soil slurry for the soil metabolome, (2) ectorhizosphere soil for DNA extraction, and (3) 24 hour hydroponic secretion for root exudates after ectorhizosphere soil removal. The schematic of EcoFAB experiment is adapted from Sasse et al. (2019).[16]

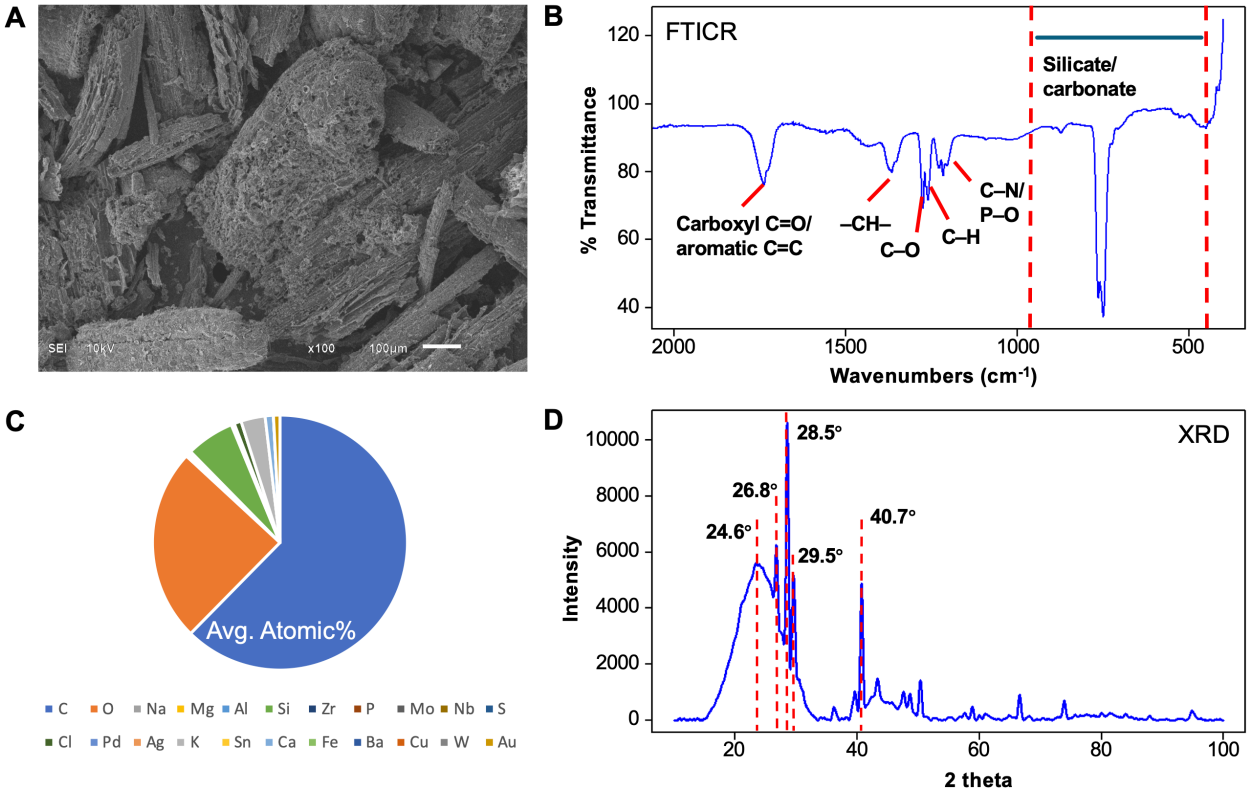

Fig 2. (A) Representative SEM image of the wheat straw biochar used in this study. (B) FTIR spectrum (400-2000 cm^{-1}) with annotations of characteristic peaks (see **Fig S2** for full spectrum image). (C) EDS-derived elemental distribution on biochar surface (atomic percentages averaged from 29 subsamples). (D) XRD spectrum with characteristic diffraction angles.

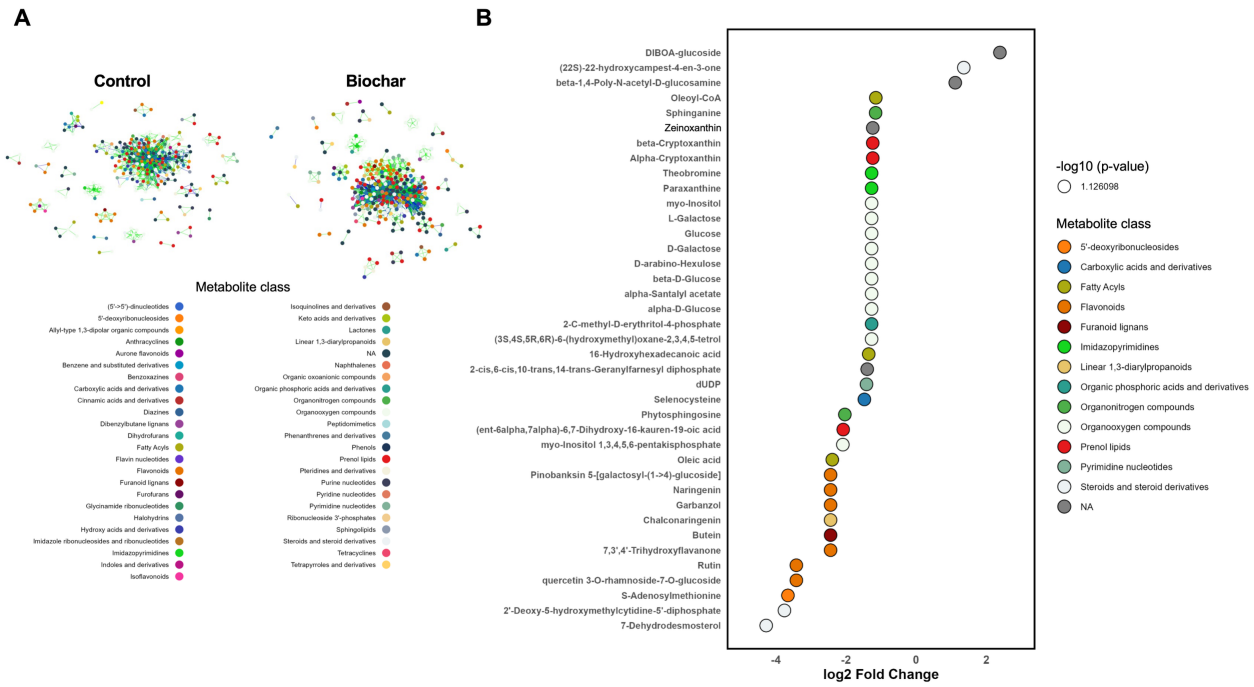

Fig 3. (A) Co-occurrence network of root exudates of the control and biochar-treated plants (r > 0.9, *p-adjusted* < 0.01). Dots indicate individual root exudates colored based on ChemOnt classes. (B) 39 most discriminative root exudates from biochar treatment ($|Log_2FC|$ > 1, *p-adjusted* < 0.05). Compounds are grouped into ChemOnt classes.

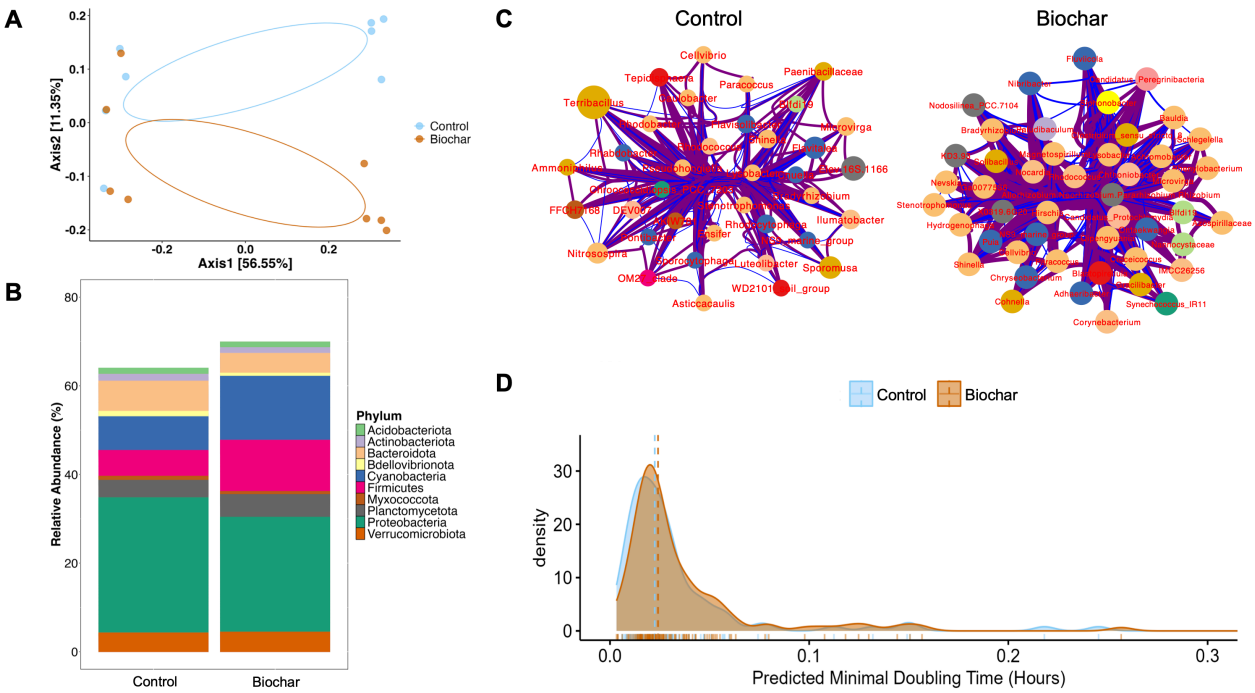

Fig 4. (A) PCoA of the native and biochar-treated rhizosphere microbiomes (PERMANOVA test: $p < 0.05$ for round x treatment). (B) Relative abundance of the top 10 microbial phyla. (C) Hub networks of keystone genera in the native and biochar-treated rhizosphere ($p < 0.05$, 1000 bootstrapping). Node colors and sizes indicate phyla and betweenness values. Purple and blue edges indicate positive and negative correlations. (D) Biochar-rewired rhizosphere microbiome had slightly slower growth rate (i.e., larger mPMDT) than the native rhizosphere microbiome based on gRodon[28,29] prediction using enriched taxa (DESeq2: $|\mathrm{Log_2FC}| > 1$, *p-adjusted* < 0.05).

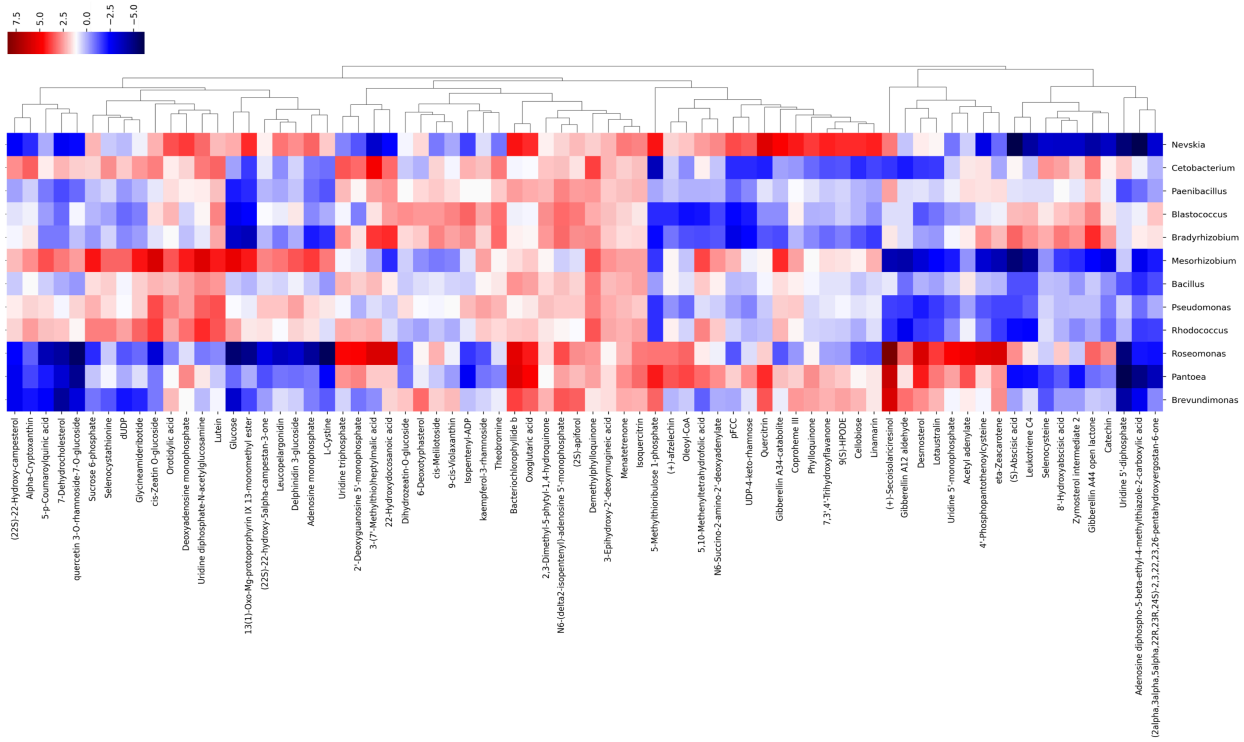

Fig 5. Associations between exudate compounds and bacterial genera inferred by the mmvec neural network.[33] Colors indicate the estimated log conditional probability of observing a root exudate compound given the presence of a microbial genus. Root exudates are clustered based on their associations with microbial genera.

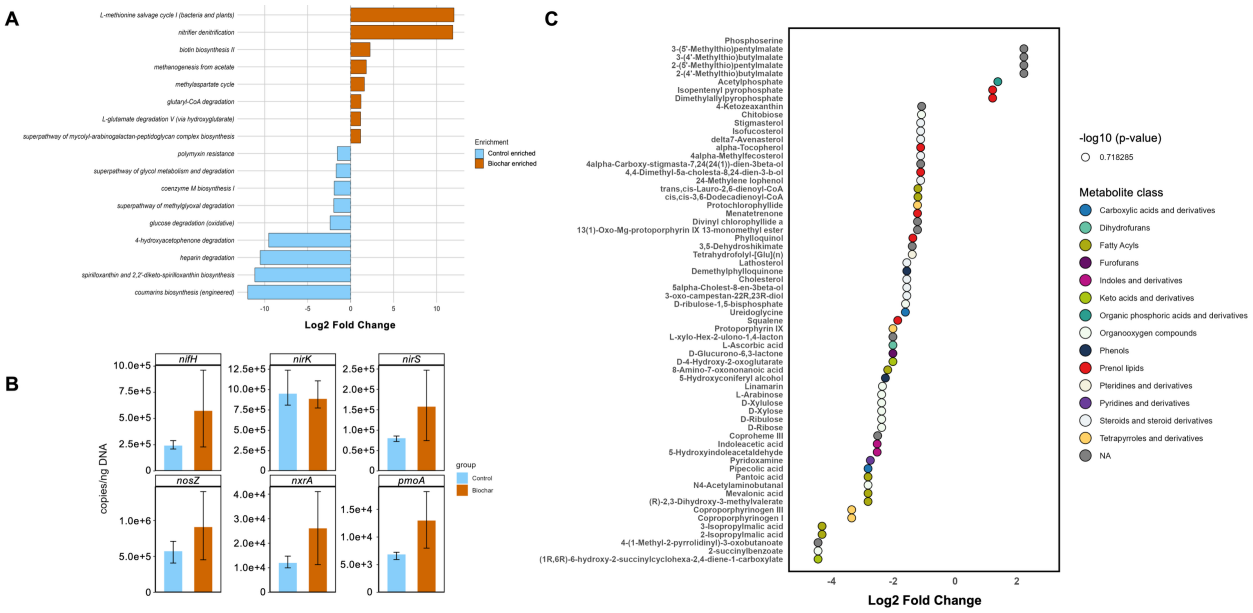

Fig 6. (A) Microbial pathways (from PICRUSt2[26]) significantly regulated by biochar ($|Log_2FC| > 1$, *p-adjusted* < 0.05). (B) Abundance of key nitrogen- and methane-cycling genes from qPCR. Boxplots represent the median and interquartile range. (C) 64 most discriminative rhizosphere soil exometabolites influenced by biochar ($|Log_2FC| > 1$, *p-adjusted* < 0.05). Compounds are grouped into ChemOnt classes.

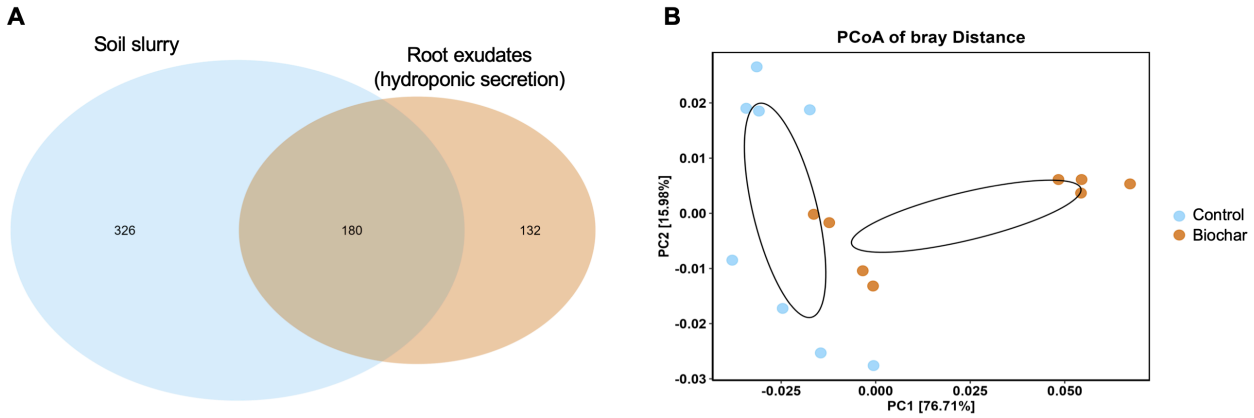

Fig 7. (A) Venn diagram showing root exudates from hydroponic secreted (312 compounds), metabolites in soils (506 compounds), and exometabolites including microbial products (326 compounds) there were detected under the biochar treatment. (B) PCoA of Bray-Curtis distance of soil metabolites detected in the control and biochar-treated rhizosphere (PERMANOVA test: p = 0.039 for experiment round; p = 0.040 for treatment). Data represents the results from two rounds of independent experiments. The ellipses represent 95% confidence.

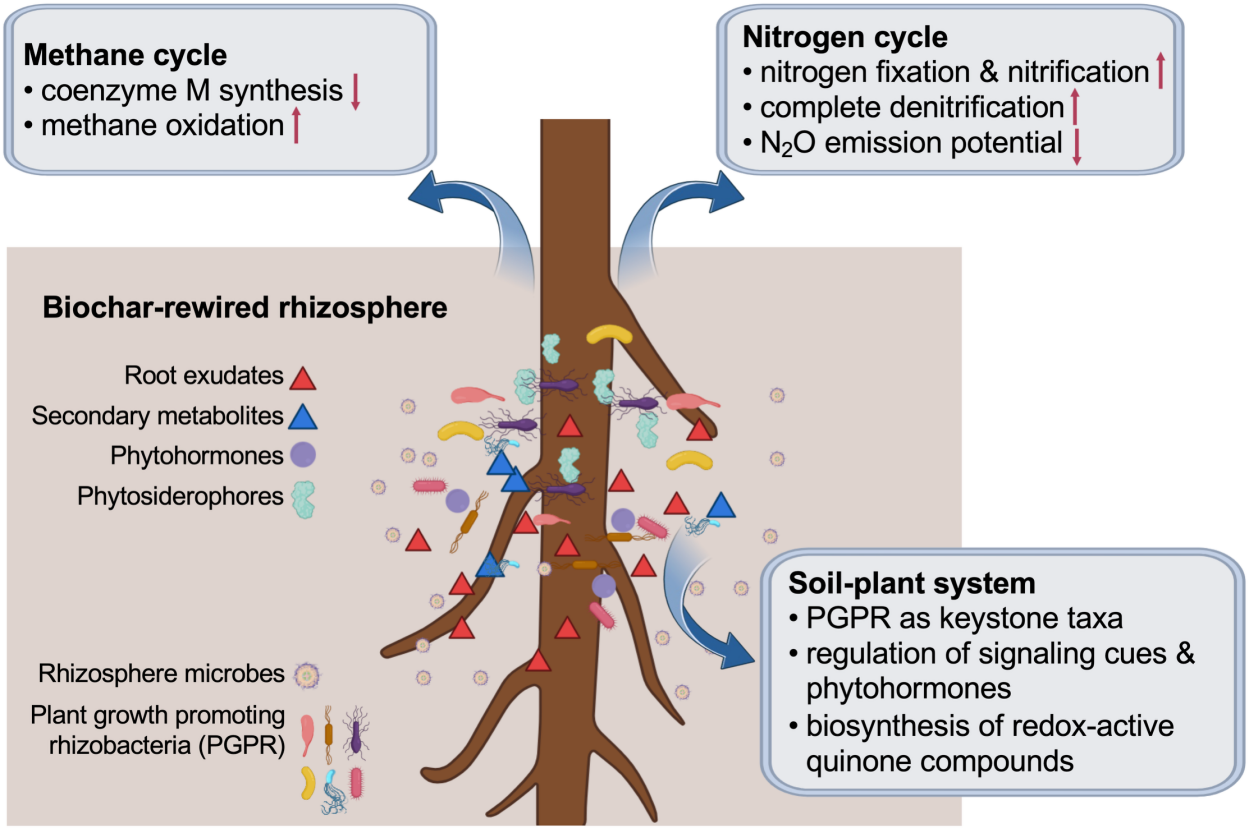
Methane cycle
• coenzyme M synthesis
• methane oxidation
Nitrogen cycle
• nitrogen fixation & nitrification
• complete denitrification
• N_2O emission potential
Biochar-rewired rhizosphere
Root exudates
Secondary metabolites
Phytohormones
Phytosiderophores
Rhizosphere microbes
Plant growth promoting rhizobacteria (PGPR)
Soil-plant system
• PGPR as keystone taxa
• regulation of signaling cues & phytohormones
• biosynthesis of redox-active quinone compounds

Graphic TOC

585 **DATA AVAILABILITY STATEMENT**

586 Raw reads are available at the NCBI Sequence Read Archive under the BioProject
587 accession number PRJNA1394313. Supporting Information tables (Table S1-S13) are also
588 available at https://doi.org/10.5281/zenodo.18930558.

589

590 **SUPPORTING INFORMATION**

591 Additional methods (biochar production and characterization, EcoFAB fabrication, plant
592 experiment and sample collection, untargeted metabolomics, next generation sequencing and
593 data processing, qPCR and data normalization, biofilm assay, multi-omics integration, general
594 statistics and data visualization), and results and discussion (characterization of wheat biochar,
595 biochar-induced differential root exudation, rhizosphere microbiome restructuring and its
596 association with biochar-induced root exudates, biochar-treated rhizosphere microbiome with
597 shifted functions) (PDF).

598 Properties of the agricultural soil and wheat biochar, qPCR primers and conditions,
599 compounds detected by Orbitrap HRMS, compounds detected in root exudates but not inside of
600 root tissues, microbes enriched in the biochar-treated or control rhizosphere, topological
601 properties of microbial co-occurrence networks reconstructed with SparCC, keystone genera
602 identified by centrality metrics (degree, betweenness, and closeness), keystone genera idefined
603 by within-module connectivity and between-module connectivity, predicted microbial pathways
604 significantly associated with biochar-induced root exudates, PICRUSt2 predicted N-cycling gene
605 abundance, PICRUSt2-predicted top 5 genera carrying denitrification genes (*narG*, *nirK*, *nirS*,
606 *nosZ*) and their relative abundance, metabolites detected only in rhizosphere soils and not in root
607 exudates, predicted microbial pathways significantly associated with biochar-induced soil
608 exometabolites (XLSX).

609

610 **AUTHOR INFORMATION**

611 **Author Contributions**

Hanyue Yang: Investigation, Methodology, Data curation, Formal analysis, Validation, Visualization, Writing – original draft, Writing – review and editing. **Amina F. Mughal:** Methodology, Formal analysis. **Yaqi You:** Conceptualization, Funding acquisition, Resources, Project administration, Supervision, Formal analysis, Validation, Visualization, Writing – review and editing.

Funding

This work was supported by the State University of New York College of Environmental Science and Forestry (SUNY ESF) through startup funds to Yaqi You. It was partially supported by the US Department of Agriculture through a McIntire-Stennis Capacity Grant (NI23MSCFRXXXG070) and the State University of New York Empire Innovation Program through its Chancellor's Early Career Scholar program. Hanyue Yang is grateful to the ESF Alumni Association.

Notes

The authors declare no competing financial interest.

ACKNOWLEDGEMENTS

We thank the group of Dr. Amin Mirkouei (University of Idaho) for producing the biochar used in this study. We would like to posthumously acknowledge Kevin Guerin (ESF Analytical and Technical Services) for great assistance with fabricating acrylic mold parts on a lathe machine. We thank Dr. Alex Artyukhin for training H. Yang on the Q Exactive HF Orbitrap mass spectrometer. We thank undergraduate students Olivia Abry and Hayden Bregg (Department of Biology, ESF) for assistance with the EcoFAB experiment, and Dr. Leanne Powers (Department of Chemistry, ESF) for assistance with DOC measurement. We are grateful to Syracuse University Research Computing for providing high-performance computing resources.

REFERENCES

(1) McConnell, L. L.; Osorio, C.; Hofmann, T. The Future of Agriculture and Food: Sustainable Approaches to Achieve Zero Hunger. *J. Agric. Food Chem.* **2023**, *71* (36), 13165–13167. https://doi.org/10.1021/acs.jafc.3c05433.

(2) Joseph, S.; Cowie, A. L.; Van Zwieten, L.; Bolan, N.; Budai, A.; Buss, W.; Cayuela, M. L.; Graber, E. R.; Ippolito, J. A.; Kuzyakov, Y.; Luo, Y.; Ok, Y. S.; Palansooriya, K. N.; Shepherd, J.; Stephens, S.; Weng, Z. (Han); Lehmann, J. How Biochar Works, and When It Doesn't: A Review of Mechanisms Controlling Soil and Plant Responses to Biochar. *GCB Bioenergy* **2021**, *13* (11), 1731–1764. https://doi.org/10.1111/gcbb.12885.

(3) Kerner, P.; Struhs, E.; Mirkouei, A.; Aho, K.; Lohse, K. A.; Dungan, R. S.; You, Y. Microbial Responses to Biochar Soil Amendment and Influential Factors: A Three-Level Meta-Analysis. *Environ. Sci. Technol.* **2023**, acs.est.3c04201. https://doi.org/10.1021/acs.est.3c04201.

(4) Uchimiya, M.; Wartelle, L. H.; Klasson, K. T.; Fortier, C. A.; Et., A. Influence of Pyrolysis Temperature on Biochar Property and Function as a Heavy Metal Sorbent in Soil. *J. Agric. Food Chem.* **2011**. https://doi.org/10.1021/jf104206c.

(5) Yang, H.; Kerner, P.; Liang, X.; Struhs, E.; Mirkouei, A.; You, Y. Biochar Amendment Modulates Root Metabolome and Rhizosphere Microbiome of Wheat. *Biochar* **2025**, *7* (1), 46. https://doi.org/10.1007/s42773-025-00434-6.

(6) Fierer, N. Embracing the Unknown: Disentangling the Complexities of the Soil Microbiome. *Nat Rev Micro* **2017**, 1–12. https://doi.org/10.1038/nrmicro.2017.87.

(7) Chen, L.; Jiang, Y.; Liang, C.; Luo, Y.; Xu, Q.; Han, C.; Zhao, Q.; Sun, B. Competitive Interaction with Keystone Taxa Induced Negative Priming under Biochar Amendments. *Microbiome* **2019**, *7* (1), 77. https://doi.org/10.1186/s40168-019-0693-7.

(8) Trivedi, P.; Leach, J. E.; Tringe, S. G.; Sa, T.; Singh, B. K. Plant–Microbiome Interactions: From Community Assembly to Plant Health. *Nat Rev Microbiol* **2020**. https://doi.org/10.1038/s41579-020-0412-1.

(9) Qu, Q.; Zhang, Z.; Peijnenburg, W. J. G. M.; Liu, W.; Lu, T.; Hu, B.; Chen, J.; Chen, J.; Lin, Z.; Qian, H. Rhizosphere Microbiome Assembly and Its Impact on Plant Growth. *J. Agric. Food Chem.* **2020**, *68* (18), 5024–5038. https://doi.org/10.1021/acs.jafc.0c00073.

(10) Klimasmith, I. M.; Kent, A. D. Micromanaging the Nitrogen Cycle in Agroecosystems. *Trends in Microbiology* **2022**, *30* (11), 1045–1055. https://doi.org/10.1016/j.tim.2022.04.006.

(11) Sun, Y.; Yue, Y.; Qian, J.; Gu, Z.; Yang, Y.; Guo, S.; Yuan, H.; Fernie, A. R. Linking Nitrate-Modulated Plant Growth and Metabolic Reprogramming to Rhizobacterial Recruitment: Insights from the Plant Metabolome and Rhizosphere Microbiome. *J. Agric. Food Chem.* **2025**, *73* (43), 27272–27287. https://doi.org/10.1021/acs.jafc.5c07233.

(12) Xiao, Z.; Rasmann, S.; Yue, L.; Lian, F.; Zou, H.; Wang, Z. The Effect of Biochar Amendment on N-Cycling Genes in Soils: A Meta-Analysis. *Science of The Total Environment* **2019**, *696*, 133984. https://doi.org/10.1016/j.scitotenv.2019.133984.

(13) Zengler, K.; Hofmockel, K.; Baliga, N. S.; Behie, S. W.; Bernstein, H. C.; Brown, J. B.; Dinneny, J. R.; Floge, S. A.; Forry, S. P.; Hess, M.; Jackson, S. A.; Jansson, C.; Lindemann,

S. R.; Pett-Ridge, J.; Maranas, C.; Venturelli, O. S.; Wallenstein, M. D.; Shank, E. A.; Northen, T. R. EcoFABs: Advancing Microbiome Science through Standardized Fabricated Ecosystems. *Nat Methods* **2019**, *16* (7), 567–571. https://doi.org/10.1038/s41592-019-0465-0.

(14) Struhs, E.; Mirkouei, A.; You, Y.; Mohajeri, A. Techno-Economic and Environmental Assessments for Nutrient-Rich Biochar Production from Cattle Manure: A Case Study in Idaho, USA. *Applied Energy* **2020**, *279*, 115782. https://doi.org/10.1016/j.apenergy.2020.115782.

(15) Gao, J.; Sasse, J.; Lewald, K. M.; Zhalnina, K.; Cornmesser, L. T.; Duncombe, T. A.; Yoshikuni, Y.; Vogel, J. P.; Firestone, M. K.; Northen, T. R. Ecosystem Fabrication (EcoFAB) Protocols for The Construction of Laboratory Ecosystems Designed to Study Plant-Microbe Interactions. *JoVE* **2018**, No. 134, 57170. https://doi.org/10.3791/57170.

(16) Sasse, J.; Kant, J.; Cole, B. J.; Klein, A. P.; Arsova, B.; Schlaepfer, P.; Gao, J.; Lewald, K.; Zhalnina, K.; Kosina, S.; Bowen, B. P.; Treen, D.; Vogel, J.; Visel, A.; Watt, M.; Dangl, J. L.; Northen, T. R. Multilab EcoFAB Study Shows Highly Reproducible Physiology and Depletion of Soil Metabolites by a Model Grass. *New Phytol* **2019**, *222* (2), 1149–1160. https://doi.org/10.1111/nph.15662.

(17) You, Y.; Kerner, P.; Shanmugam, S.; Khodakovskaya, M. V. Emerging Investigator Series: Differential Effects of Carbon Nanotubes and Graphene on the Tomato Rhizosphere Microbiome. *Environ. Sci.: Nano* **2023**, 10.1039.D2EN01026G. https://doi.org/10.1039/D2EN01026G.

(18) Yang, H.; Wang, C.; Chen, F.; Yue, L.; Cao, X.; Li, J.; Zhao, X.; Wu, F.; Wang, Z.; Xing, B. Foliar Carbon Dot Amendment Modulates Carbohydrate Metabolism, Rhizospheric Properties and Drought Tolerance in Maize Seedling. *Science of The Total Environment* **2022**, *809*, 151105. https://doi.org/10.1016/j.scitotenv.2021.151105.

(19) Pang, Z.; Zhou, G.; Ewald, J.; Chang, L.; Hacariz, O.; Basu, N.; Xia, J. Using MetaboAnalyst 5.0 for LC–HRMS Spectra Processing, Multi-Omics Integration and Covariate Adjustment of Global Metabolomics Data. *Nat Protoc* **2022**, *17* (8), 1735–1761. https://doi.org/10.1038/s41596-022-00710-w.

(20) Schmid, R.; Heuckeroth, S.; Korf, A.; Smirnov, A.; Myers, O.; Dyrlund, T. S.; Bushuiev, R.; Murray, K. J.; Hoffmann, N.; Lu, M.; Sarvepalli, A.; Zhang, Z.; Fleischauer, M.; Dührkop, K.; Wesner, M.; Hoogstra, S. J.; Rudt, E.; Mokshyna, O.; Brungs, C.; Ponomarov, K.; Mutabdžija, L.; Damiani, T.; Pudney, C. J.; Earll, M.; Helmer, P. O.; Fallon, T. R.; Schulze, T.; Rivas-Ubach, A.; Bilbao, A.; Richter, H.; Nothias, L.-F.; Wang, M.; Orešič, M.; Weng, J.-K.; Böcker, S.; Jeibmann, A.; Hayen, H.; Karst, U.; Dorrestein, P. C.; Petras, D.; Du, X.; Pluskal, T. Integrative Analysis of Multimodal Mass Spectrometry Data in MZmine 3. *Nat Biotechnol* **2023**, *41* (4), 447–449. https://doi.org/10.1038/s41587-023-01690-2.

(21) Huan, T.; Forsberg, E. M.; Rinehart, D.; Johnson, C. H.; Ivanisevic, J.; Benton, H. P.; Fang, M.; Aisporna, A.; Hilmers, B.; Poole, F. L.; Thorgersen, M. P.; Adams, M. W. W.; Krantz, G.; Fields, M. W.; Robbins, P. D.; Niedernhofer, L. J.; Ideker, T.; Majumder, E. L.; Wall, J. D.; Rattray, N. J. W.; Goodacre, R.; Lairson, L. L.; Siuzdak, G. Systems Biology Guided by

XCMS Online Metabolomics. *Nat Chem Biol* **2017**, *14* (5), 461–462. https://doi.org/10.1038/nmeth.4260.

(22) Djoumbou Feunang, Y.; Eisner, R.; Knox, C.; Chepelev, L.; Hastings, J.; Owen, G.; Fahy, E.; Steinbeck, C.; Subramanian, S.; Bolton, E.; Greiner, R.; Wishart, D. S. ClassyFire: Automated Chemical Classification with a Comprehensive, Computable Taxonomy. *J Cheminform* **2016**, *8* (1), 61. https://doi.org/10.1186/s13321-016-0174-y.

(23) Bolyen, E.; Rideout, J. R.; Dillon, M. R.; Bokulich, N. A.; Abnet, C. C.; Al-Ghalith, G. A.; Alexander, H.; Alm, E. J.; Arumugam, M.; Asnicar, F.; Bai, Y.; Bisanz, J. E.; Bittinger, K.; Brejnrod, A.; Brislawn, C. J.; Brown, C. T.; Callahan, B. J.; guez, A. x000E9 s M. C.-R. x000ED; Chase, J.; Cope, E. K.; Silva, R.; Diener, C.; Dorrestein, P. C.; Douglas, G. M.; Durall, D. M.; Duvallet, C.; Edwardson, C. F.; Ernst, M.; Estaki, M.; Fouquier, J.; Gauglitz, J. M.; Gibbons, S. M.; Gibson, D. L.; Gonzalez, A.; Gorlick, K.; Guo, J.; Hillmann, B.; Holmes, S.; Holste, H.; Huttenhower, C.; Huttley, G. A.; Janssen, S.; Jarmusch, A. K.; Jiang, L.; Kaehler, B. D.; Bin Kang, K.; Keefe, C. R.; Keim, P.; Kelley, S. T.; Knights, D.; Koester, I.; Kosciolek, T.; Kreps, J.; Langille, M. G. I.; Lee, J.; Ley, R.; Liu, Y.-X.; Loftfield, E.; Lozupone, C.; Maher, M.; Marotz, C.; Martin, B. D.; McDonald, D.; McIver, L. J.; Melnik, A. V.; Metcalf, J. L.; Morgan, S. C.; Morton, J. T.; Naimey, A. T.; Navas-Molina, J. A.; Nothias, L. F.; Orchanian, S. B.; Pearson, T.; Peoples, S. L.; Petras, D.; Preuss, M. L.; Pruesse, E.; Rasmussen, L. B.; Rivers, A.; Robeson, M. S.; Rosenthal, P.; Segata, N.; Shaffer, M.; Shiffer, A.; Sinha, R.; Song, S. J.; Spear, J. R.; Swafford, A. D.; Thompson, L. R.; Torres, P. J.; Trinh, P.; Tripathi, A.; Turnbaugh, P. J.; Ul-Hasan, S.; Hooft, J. J. J.; Vargas, F.; zquez-Baeza, Y. V. x000E1; Vogtmann, E.; von Hippel, M.; Walters, W.; Wan, Y.; Wang, M.; Warren, J.; Weber, K. C.; Williamson, C. H. D.; Willis, A. D.; Xu, Z. Z.; Zaneveld, J. R.; Zhang, Y.; Zhu, Q.; Knight, R.; Caporaso, J. G. Reproducible, Interactive, Scalable and Extensible Microbiome Data Science Using QIIME 2. *Nature Biotechnology* **2019**, 1–6. https://doi.org/10.1038/s41587-019-0209-9.

(24) Callahan, B. J.; McMurdie, P. J.; Rosen, M. J.; Han, A. W.; Johnson, A. J. A.; Holmes, S. P. DADA2: High-Resolution Sample Inference from Illumina Amplicon Data. *Nat Methods* **2016**, *13* (7), 581–583. https://doi.org/10.1038/nmeth.3869.

(25) McMurdie, P. J.; Holmes, S. Phyloseq: An R Package for Reproducible Interactive Analysis and Graphics of Microbiome Census Data. *PLoS ONE* **2013**, *8* (4), e61217-11. https://doi.org/10.1371/journal.pone.0061217.

(26) Douglas, G. M.; Maffei, V. J.; Zaneveld, J. R.; Yurgel, S. N.; Brown, J. R.; Taylor, C. M.; Huttenhower, C.; Langille, M. G. I. PICRUSt2 for Prediction of Metagenome Functions. *Nat Biotechnol* **2020**, *38* (6), 685–688. https://doi.org/10.1038/s41587-020-0548-6.

(27) Yang, C.; Mai, J.; Cao, X.; Burberry, A.; Cominelli, F.; Zhang, L. Ggpicrust2: An R Package for PICRUSt2 Predicted Functional Profile Analysis and Visualization. *Bioinformatics* **2023**, *39* (8), btad470. https://doi.org/10.1093/bioinformatics/btad470.

(28) Weissman, J. L.; Hou, S.; Fuhrman, J. A. Estimating Maximal Microbial Growth Rates from Cultures, Metagenomes, and Single Cells via Codon Usage Patterns. *Proc. Natl. Acad. Sci. U.S.A.* **2021**, *118* (12), e2016810118. https://doi.org/10.1073/pnas.2016810118.

(29) López, J. L.; Fourie, A.; Poppeliers, S. W. M.; Pappas, N.; Sánchez-Gil, J. J.; De Jonge, R.; Dutilh, B. E. Growth Rate Is a Dominant Factor Predicting the Rhizosphere Effect. *ISME J* **2023**, *17* (9), 1396–1405. https://doi.org/10.1038/s41396-023-01453-6.

(30) Friedman, J.; Alm, E. J. Inferring Correlation Networks from Genomic Survey Data. *PLoS Comput Biol* **2012**.

(31) Ning, D.; Wang, Y.; Fan, Y.; Wang, J.; Van Nostrand, J. D.; Wu, L.; Zhang, P.; Curtis, D. J.; Tian, R.; Lui, L.; Hazen, T. C.; Alm, E. J.; Fields, M. W.; Poole, F.; Adams, M. W. W.; Chakraborty, R.; Stahl, D. A.; Adams, P. D.; Arkin, A. P.; He, Z.; Zhou, J. Environmental Stress Mediates Groundwater Microbial Community Assembly. *Nat Microbiol* **2024**, *9* (2), 490–501. https://doi.org/10.1038/s41564-023-01573-x.

(32) Stegen, J. C.; Lin, X.; Fredrickson, J. K.; Chen, X.; Kennedy, D. W.; Murray, C. J.; Rockhold, M. L.; Konopka, A. Quantifying Community Assembly Processes and Identifying Features That Impose Them. *ISME J* **2013**, *7* (11), 2069–2079. https://doi.org/10.1038/ismej.2013.93.

(33) Morton, J. T.; Aksenov, A. A.; Nothias, L. F.; Foulds, J. R.; Quinn, R. A.; Badri, M. H.; Swenson, T. L.; Goethem, M. W.; Northen, T. R.; Vázquez-Baeza, Y.; Wang, M.; Bokulich, N. A.; Watters, A.; Song, S. J.; Bonneau, R.; Dorrestein, P. C.; Knight, R. Learning Representations of Microbe–Metabolite Interactions. *Nat Chem Biol* **2019**, 1–12. https://doi.org/10.1038/s41592-019-0616-3.

(34) Zhou, G.; Pang, Z.; Lu, Y.; Ewald, J.; Xia, J. OmicsNet 2.0: A Web-Based Platform for Multi-Omics Integration and Network Visual Analytics. *Nucleic Acids Research* **2022**, *50* (W1), W527–W533. https://doi.org/10.1093/nar/gkac376.

(35) Liu, L.; Liu, G.; Zhou, J.; Wang, J.; Jin, R.; Wang, A. Improved Bioreduction of Nitrobenzene by Black Carbon/Biochar Derived from Crop Residues. *RSC Adv.* **2016**, *6* (87), 84388–84396. https://doi.org/10.1039/C6RA11671J.

(36) Yao, S.; Li, X.; Cheng, H.; Zhang, C.; Bian, Y.; Jiang, X.; Song, Y. Resource Utilization of a Typical Vegetable Waste as Biochars in Removing Phthalate Acid Esters from Water: A Sorption Case Study. *Bioresource Technology* **2019**, *293*, 122081. https://doi.org/10.1016/j.biortech.2019.122081.

(37) Waqas, M.; Aburiazaiza, A. S.; Miandad, R.; Rehan, M.; Barakat, M. A.; Nizami, A. S. Development of Biochar as Fuel and Catalyst in Energy Recovery Technologies. *Journal of Cleaner Production* **2018**, *188*, 477–488. https://doi.org/10.1016/j.jclepro.2018.04.017.

(38) Vukašinović, N.; Wang, Y.; Vanhoutte, I.; Fendrych, M.; Guo, B.; Kvasnica, M.; Jiroutová, P.; Oklestkova, J.; Strnad, M.; Russinova, E. Local Brassinosteroid Biosynthesis Enables Optimal Root Growth. *Nat. Plants* **2021**, *7* (5), 619–632. https://doi.org/10.1038/s41477-021-00917-x.

(39) Hazrati, H.; Fomsgaard, I. S.; Kudsk, P. Root-Exuded Benzoxazinoids: Uptake and Translocation in Neighboring Plants. *J. Agric. Food Chem.* **2020**, *68* (39), 10609–10617. https://doi.org/10.1021/acs.jafc.0c04245.

(40) Hu, L.; Robert, C. A. M.; Cadot, S.; Zhang, X.; Ye, M.; Li, B.; Manzo, D.; Chervet, N.; Steinger, T.; van der Heijden, M. G. A.; Schlaeppi, K.; Erb, M. Root Exudate Metabolites Drive Plant-Soil Feedbacks on Growth and Defense by Shaping the Rhizosphere

Microbiota. *Nat Commun* **2018**, *9* (1), 2738. https://doi.org/10.1038/s41467-018-05122-7.

(41) Yu, J.; Tu, X.; Huang, A. C. Functions and Biosynthesis of Plant Signaling Metabolites Mediating Plant–Microbe Interactions. *Nat. Prod. Rep.* **2022**, *39* (7), 1393–1422. https://doi.org/10.1039/D2NP00010E.

(42) Beck, J. J.; Alborn, H. T.; Block, A. K.; Christensen, S. A.; Et., A. Interactions Among Plants, Insects, and Microbes: Elucidation of Inter-Organismal Chemical Communications in Agricultural Ecology. *J. Agric. Food Chem.* **2018**. https://doi.org/10.1021/acs.jafc.8b01763.

(43) Kudjordjie, E. N.; Sapkota, R.; Steffensen, S. K.; Fomsgaard, I. S.; Nicolaisen, M. Maize Synthesized Benzoxazinoids Affect the Host Associated Microbiome. *Microbiome* **2019**, *7* (1), 59. https://doi.org/10.1186/s40168-019-0677-7.

(44) Chen, K.-J.; Zheng, Y.-Q.; Kong, C.-H.; Zhang, S.-Z.; Li, J.; Liu, X.-G. 2,4-Dihydroxy-7-Methoxy-1,4-Benzoxazin-3-One (DIMBOA) and 6-Methoxy-Benzoxazolin-2-One (MBOA) Levels in the Wheat Rhizosphere and Their Effect on the Soil Microbial Community Structure. *J. Agric. Food Chem.* **2010**, *58* (24), 12710–12716. https://doi.org/10.1021/jf1032608.

(45) Wang, L.; Chen, M.; Lam, P.-Y.; Dini-Andreote, F.; Dai, L.; Wei, Z. Multifaceted Roles of Flavonoids Mediating Plant-Microbe Interactions. *Microbiome* **2022**, *10* (1), 233. https://doi.org/10.1186/s40168-022-01420-x.

(46) Liang, T.; Shi, C.; Peng, Y.; Tan, H.; Xin, P.; Yang, Y.; Wang, F.; Li, X.; Chu, J.; Huang, J.; Yin, Y.; Liu, H. Brassinosteroid-Activated BRI1-EMS-SUPPRESSOR 1 Inhibits Flavonoid Biosynthesis and Coordinates Growth and UV-B Stress Responses in Plants. *Plant Cell* **2020**, *32* (10), 3224–3239. https://doi.org/10.1105/tpc.20.00048.

(47) Biederman, L. A.; Harpole, W. S. Biochar and Its Effects on Plant Productivity and Nutrient Cycling: A Meta-Analysis. *GCB Bioenergy* **2013**, *5* (2), 202–214. https://doi.org/10.1111/gcbb.12037.

(48) Macabuhay, A.; Arsova, B.; Walker, R.; Johnson, A.; Watt, M.; Roessner, U. Modulators or Facilitators? Roles of Lipids in Plant Root–Microbe Interactions. *Trends in Plant Science* **2022**, *27* (2), 180–190. https://doi.org/10.1016/j.tplants.2021.08.004.

(49) He, M.; Ding, N.-Z. Plant Unsaturated Fatty Acids: Multiple Roles in Stress Response. *Front. Plant Sci.* **2020**, *11*. https://doi.org/10.3389/fpls.2020.562785.

(50) Gu, S.; Wei, Z.; Shao, Z.; Friman, V.-P.; Cao, K.; Yang, T.; Kramer, J.; Wang, X.; Li, M.; Mei, X.; Xu, Y.; Shen, Q.; Kümmerli, R.; Jousset, A. Competition for Iron Drives Phytopathogen Control by Natural Rhizosphere Microbiomes. *Nat Microbiol* **2020**, *5* (8), 1002–1010. https://doi.org/10.1038/s41564-020-0719-8.

(51) O'Banion, B. S.; Jones, P.; Demetros, A. A.; Kelley, B. R.; Knoor, L. H.; Wagner, A. S.; Chen, J.-G.; Muchero, W.; Reynolds, T. B.; Jacobson, D.; Lebeis, S. L. Plant Myo-Inositol Transport Influences Bacterial Colonization Phenotypes. *Current Biology* **2023**, *33* (15), 3111-3124.e5. https://doi.org/10.1016/j.cub.2023.06.057.

(52) Orozco-Mosqueda, Ma. D. C.; Santoyo, G.; Glick, B. R. Recent Advances in the Bacterial Phytohormone Modulation of Plant Growth. *Plants* **2023**, *12* (3), 606. https://doi.org/10.3390/plants12030606.

(53) Hollensteiner, J.; Schneider, D.; Poehlein, A.; Brinkhoff, T.; Daniel, R. Pan-Genome Analysis of Six Paracoccus Type Strain Genomes Reveal Lifestyle Traits. *PLoS ONE* **2023**, *18* (12), e0287947. https://doi.org/10.1371/journal.pone.0287947.
(54) De Bruijn, I.; Cheng, X.; De Jager, V.; Expósito, R. G.; Watrous, J.; Patel, N.; Postma, J.; Dorrestein, P. C.; Kobayashi, D.; Raaijmakers, J. M. Comparative Genomics and Metabolic Profiling of the Genus Lysobacter. *BMC Genomics* **2015**, *16* (1), 991. https://doi.org/10.1186/s12864-015-2191-z.
(55) Kumar, A.; Rithesh, L.; Kumar, V.; Raghuvanshi, N.; Chaudhary, K.; Abhineet; Pandey, A. K. Stenotrophomonas in Diversified Cropping Systems: Friend or Foe? *Front. Microbiol.* **2023**, *14*, 1214680. https://doi.org/10.3389/fmicb.2023.1214680.
(56) Wang, Z.; Hu, H.; Zhang, Z.; Xu, Y.; Xu, P.; Tang, H. IA Multiple PAHs-Degrading Shinella Sp. Strain and Its Potential Bioremediation in Wastewater. *Science of The Total Environment* **2023**, *879*, 162974. https://doi.org/10.1016/j.scitotenv.2023.162974.
(57) Forsberg, Z.; Nelson, C. E.; Dalhus, B.; Mekasha, S.; Loose, J. S. M.; Crouch, L. I.; Røhr, Å. K.; Gardner, J. G.; Eijsink, V. G. H.; Vaaje-Kolstad, G. Structural and Functional Analysis of a Lytic Polysaccharide Monooxygenase Important for Efficient Utilization of Chitin in Cellvibrio Japonicus. *Journal of Biological Chemistry* **2016**, *291* (14), 7300–7312. https://doi.org/10.1074/jbc.M115.700161.
(58) Ma, S.; Huang, S.; Tian, Y.; Lu, X. Heterotrophic Ammonium Assimilation: An Important Driving Force for Aerobic Denitrification of Rhodococcus Erythropolis Strain Y10. *Chemosphere* **2022**, *291*, 132910. https://doi.org/10.1016/j.chemosphere.2021.132910.
(59) Yuzikhin, O. S.; Gogoleva, N. E.; Shaposhnikov, A. I.; Konnova, T. A.; Osipova, E. V.; Syrova, D. S.; Ermakova, E. A.; Shevchenko, V. P.; Nagaev, I. Yu.; Shevchenko, K. V.; Myasoedov, N. F.; Safronova, V. I.; Shavarda, A. L.; Nizhnikov, A. A.; Belimov, A. A.; Gogolev, Y. V. Rhizosphere Bacterium Rhodococcus Sp. P1Y Metabolizes Abscisic Acid to Form Dehydrovomifoliol. *Biomolecules* **2021**, *11* (3), 345. https://doi.org/10.3390/biom11030345.
(60) Jara-Servin, A.; Mejia, G.; Romero, M. F.; Peimbert, M.; Alcaraz, L. D. Unravelling the Genomic and Environmental Diversity of the Ubiquitous Solirubrobacter. *Environmental Microbiology* **2024**, *26* (8), e16685. https://doi.org/10.1111/1462-2920.16685.
(61) Jung, H.; Lee, D.; Lee, S.; Kong, H. J.; Park, J.; Seo, Y.-S. Comparative Genomic Analysis of Chryseobacterium Species: Deep Insights into Plant-Growth-Promoting and Halotolerant Capacities. *Microbial Genomics* **2023**, *9* (10). https://doi.org/10.1099/mgen.0.001108.
(62) Zhang, C.; Zhou, D.-F.; Wang, M.-Y.; Song, Y.-Z.; Zhang, C.; Zhang, M.-M.; Sun, J.; Yao, L.; Mo, X.-H.; Ma, Z.-X.; Yuan, X.-J.; Shao, Y.; Wang, H.-R.; Dong, S.-H.; Bao, K.; Lu, S.-H.; Sadilek, M.; Kalyuzhnaya, M. G.; Xing, X.-H.; Yang, S. Phosphoribosylpyrophosphate Synthetase as a Metabolic Valve Advances Methylobacterium/Methylorubrum Phyllosphere Colonization and Plant Growth. *Nat Commun* **2024**, *15* (1). https://doi.org/10.1038/s41467-024-50342-9.
(63) Lu, Y.; Rosencrantz, D.; Liesack, W.; Conrad, R. Structure and Activity of Bacterial Community Inhabiting Rice Roots and the Rhizosphere. *Environmental Microbiology* **2006**, *8*

(8), 1351–1360. https://doi.org/10.1111/j.1462-2920.2006.01028.x.
(64) Alotaibi, F.; St-Arnaud, M.; Hijri, M. In-Depth Characterization of Plant Growth Promotion Potentials of Selected Alkanes-Degrading Plant Growth-Promoting Bacterial Isolates. *Front. Microbiol.* **2022**, *13*, 863702. https://doi.org/10.3389/fmicb.2022.863702.
(65) Ludington, W. B.; Seher, T. D.; Applegate, O.; Li, X.; Kliegman, J. I.; Langelier, C.; Atwill, E. R.; Harter, T.; DeRisi, J. L. Assessing Biosynthetic Potential of Agricultural Groundwater through Metagenomic Sequencing: A Diverse Anammox Community Dominates Nitrate-Rich Groundwater. *PLoS ONE* **2017**, *12* (4), e0174930. https://doi.org/10.1371/journal.pone.0174930.
(66) Radhakrishnan, N.; Krishnasamy, C. Isolation and Characterization of Salt-Stress-Tolerant Rhizosphere Soil Bacteria and Their Effects on Plant Growth-Promoting Properties. *Sci Rep* **2024**, *14* (1), 24909. https://doi.org/10.1038/s41598-024-75022-y.
(67) Venturi, V.; Keel, C. Signaling in the Rhizosphere. *Trends in Plant Science* **2016**, *21* (3), 187–198. https://doi.org/10.1016/j.tplants.2016.01.005.
(68) Marschmann, G. L.; Tang, J.; Zhalnina, K.; Karaoz, U.; Cho, H.; Le, B.; Pett-Ridge, J.; Brodie, E. L. Predictions of Rhizosphere Microbiome Dynamics with a Genome-Informed and Trait-Based Energy Budget Model. *Nat Microbiol* **2024**, *9* (2), 421–433. https://doi.org/10.1038/s41564-023-01582-w.
(69) Thoenen, L.; Giroud, C.; Kreuzer, M.; Waelchli, J.; Gfeller, V.; Deslandes-Hérold, G.; Mateo, P.; Robert, C. A. M.; Ahrens, C. H.; Rubio-Somoza, I.; Bruggmann, R.; Erb, M.; Schlaeppi, K. Bacterial Tolerance to Host-Exuded Specialized Metabolites Structures the Maize Root Microbiome. *Proc. Natl. Acad. Sci. U.S.A.* **2023**, *120* (44), e2310134120. https://doi.org/10.1073/pnas.2310134120.
(70) Zhalnina, K.; Louie, K. B.; Hao, Z.; Mansoori, N.; da Rocha, U. N.; Shi, S.; Cho, H.; Karaoz, U.; Loqué, D.; Bowen, B. P.; Firestone, M. K.; Northen, T. R.; Brodie, E. L. Dynamic Root Exudate Chemistry and Microbial Substrate Preferences Drive Patterns in Rhizosphere Microbial Community Assembly. *Nat Microbiol* **2018**, *3* (4), 470–480. https://doi.org/10.1038/s41564-018-0129-3.
(71) Nascimento, F. X.; Hernandez, A. G.; Glick, B. R.; Rossi, M. J. The Extreme Plant-growth-promoting Properties of *Pantoea Phytobeneficialis* MSR2 Revealed by Functional and Genomic Analysis. *Environmental Microbiology* **2020**, *22* (4), 1341–1355. https://doi.org/10.1111/1462-2920.14946.
(72) Hartmann, M.; Six, J. Soil Structure and Microbiome Functions in Agroecosystems. *Nat Rev Earth Environ* **2022**, *4* (1), 4–18. https://doi.org/10.1038/s43017-022-00366-w.
(73) Nett, R. S.; Contreras, T.; Peters, R. J. Characterization of CYP115 As a Gibberellin 3-Oxidase Indicates That Certain Rhizobia Can Produce Bioactive Gibberellin A_4. *ACS Chem. Biol.* **2017**, *12* (4), 912–917. https://doi.org/10.1021/acschembio.6b01038.
(74) Nett, R. S.; Montanares, M.; Marcassa, A.; Lu, X.; Nagel, R.; Charles, T. C.; Hedden, P.; Rojas, M. C.; Peters, R. J. Elucidation of Gibberellin Biosynthesis in Bacteria Reveals Convergent Evolution. *Nat Chem Biol* **2017**, *13* (1), 69–74. https://doi.org/10.1038/nchembio.2232.

(75) Pertry, I.; Václavíková, K.; Depuydt, S.; Galuszka, P.; Spíchal, L.; Temmerman, W.; Stes, E.; Schmülling, T.; Kakimoto, T.; Van Montagu, M. C. E.; Strnad, M.; Holsters, M.; Tarkowski, P.; Vereecke, D. Identification of *Rhodococcus Fascians* Cytokinins and Their Modus Operandi to Reshape the Plant. *Proc. Natl. Acad. Sci. U.S.A.* **2009**, *106* (3), 929–934. https://doi.org/10.1073/pnas.0811683106.

(76) Yin, L.-Z.; Li, J.-L.; Fang, B.-Z.; Liu, Z.-T.; Wang, P.; Dong, L.; Duan, L.; Luo, X.-Q.; Li, S.-H.; Li, W.-J. Roseomonas Ponticola Sp. Nov., a Novel Bacterium Isolated from Pearl River Estuary. *International Journal of Systematic and Evolutionary Microbiology* **2021**, *71* (10). https://doi.org/10.1099/ijsem.0.004994.

(77) Zhang, X.; Qiu, Y.; Gilliam, F. S.; Gillespie, C. J.; Tu, C.; Reberg-Horton, S. C.; Hu, S. Arbuscular Mycorrhizae Shift Community Composition of N-Cycling Microbes and Suppress Soil N_2O Emission. *Environ. Sci. Technol.* **2022**, *56* (18), 13461–13472. https://doi.org/10.1021/acs.est.2c03816.

(78) Cayuela, M. L.; Sánchez-Monedero, M. A.; Roig, A.; Hanley, K.; Enders, A.; Lehmann, J. Biochar and Denitrification in Soils: When, How Much and Why Does Biochar Reduce N2O Emissions? *Sci Rep* **2013**, *3* (1), 1732. https://doi.org/10.1038/srep01732.

(79) Shan, J.; Sanford, R. A.; Chee-Sanford, J.; Ooi, S. K.; Löffler, F. E.; Konstantinidis, K. T.; Yang, W. H. Beyond Denitrification: The Role of Microbial Diversity in Controlling Nitrous Oxide Reduction and Soil Nitrous Oxide Emissions. *Glob Change Biol* **2021**, *27* (12), 2669–2683. https://doi.org/10.1111/gcb.15545.

(80) Li, Y.; Katzmann, E.; Borg, S.; Schüler, D. The Periplasmic Nitrate Reductase Nap Is Required for Anaerobic Growth and Involved in Redox Control of Magnetite Biomineralization in Magnetospirillum Gryphiswaldense. *J Bacteriol* **2012**, *194* (18), 4847–4856. https://doi.org/10.1128/JB.00903-12.

(81) He, G.; Wang, W.; Chen, G.; Xie, Y.; Parks, J. M.; Davin, M. E.; Hettich, R. L.; Konstantinidis, K. T.; Löffler, F. E. A Novel Bacterial Protein Family That Catalyses Nitrous Oxide Reduction. *Nature* **2025**, *646* (8083), 152–160. https://doi.org/10.1038/s41586-025-09401-4.

(82) Garcia, P. S.; Gribaldo, S.; Borrel, G. Diversity and Evolution of Methane-Related Pathways in Archaea. *Annu. Rev. Microbiol.* **2022**, *76* (1), 727–755. https://doi.org/10.1146/annurev-micro-041020-024935.

(83) Nazaries, L.; Murrell, J. C.; Millard, P.; Baggs, L.; Singh, B. K. Methane, Microbes and Models: Fundamental Understanding of the Soil Methane Cycle for Future Predictions. *Environmental Microbiology* **2013**, *15* (9), 2395–2417. https://doi.org/10.1111/1462-2920.12149.

(84) Bueno De Mesquita, C. P.; Wu, D.; Tringe, S. G. Methyl-Based Methanogenesis: An Ecological and Genomic Review. *Microbiol Mol Biol Rev* **2023**, *87* (1), e00024-22. https://doi.org/10.1128/mmbr.00024-22.

(85) Sekowska, A.; Ashida, H.; Danchin, A. Revisiting the Methionine Salvage Pathway and Its Paralogues. *Microbial Biotechnology* **2019**, *12* (1), 77–97. https://doi.org/10.1111/1751-7915.13324.

(86) Li, X.; Bei, Q.; Rabiei Nematabad, M.; Peng, J.; Liesack, W. Time-Shifted Expression of Acetoclastic and Methylotrophic Methanogenesis by a Single Methanosarcina Genomospecies Predominates the Methanogen Dynamics in Philippine Rice Field Soil. *Microbiome* **2024**, *12* (1), 39. https://doi.org/10.1186/s40168-023-01739-z.

(87) Paul, R.; Bechtold, E. K.; Ellenbogen, J.; Woyda, R.; Holloway, T.; Carter, N.; Heslop-Harrison, G.; Wrighton, K. C.; Wilkins, M. J. Methyl-Processing Metabolisms Play Central Roles in Methane Cycling during Rice Cultivation. *Agriculture, Ecosystems & Environment* **2026**, *395*, 109952. https://doi.org/10.1016/j.agee.2025.109952.

(88) Beblawy, S.; Bursac, T.; Paquete, C.; Louro, R.; Clarke, T. A.; Gescher, J. Extracellular Reduction of Solid Electron Acceptors by *Shewanella Oneidensis*. *Molecular Microbiology* **2018**, *109* (5), 571–583. https://doi.org/10.1111/mmi.14067.

(89) Moscoviz, R.; Quéméner, E. D.-L.; Trably, E.; Bernet, N.; Hamelin, J. Novel Outlook in Microbial Ecology: Nonmutualistic Interspecies Electron Transfer. *Trends in Microbiology* **2020**, *28* (4), 245–253. https://doi.org/10.1016/j.tim.2020.01.008.

(90) Yang, S.; Liu, H.; Xie, P.; Wen, T.; Shen, Q.; Yuan, J. Emerging Pathways for Engineering the Rhizosphere Microbiome for Optimal Plant Health. *J. Agric. Food Chem.* **2023**, *71* (11), 4441–4449. https://doi.org/10.1021/acs.jafc.2c08758.

(91) Capanoglu, E.; Nemli, E.; Tomas-Barberan, F. Novel Approaches in the Valorization of Agricultural Wastes and Their Applications. *J. Agric. Food Chem.* **2022**, *70* (23), 6787–6804. https://doi.org/10.1021/acs.jafc.1c07104.